Illuminating Economic Growth *

Yingyao Hu[†]   Jiaxiong Yao[‡]

July 13, 2019

Abstract

This paper seeks to illuminate official measures of real GDP per capita using satellite-recorded nighttime lights in a measurement error model framework. Using recently developed results, we identify and estimate the nonlinear relationship between nighttime lights and true GDP per capita, as well as the nonparametric distribution of errors in official measures. We obtain three key results: (i) elasticities of nighttime lights to real GDP are between 0 and 2.3 depending on countries' income levels; (ii) GDP per capita measures are less precise for low and middle income countries, and nighttime lights can play a bigger role in improving such measures; (iii) our new measures of GDP, based on optimal combination of nighttime lights and official data, imply that some countries' real GDP growth may systematically differ from official data.

Keywords: Nighttime lights, measurement error, GDP per capita, elasticity

1   Introduction

Real Gross Domestic Product (GDP) is at the heart of macroeconomic analysis and policy-making. It is the basis for measuring national economic development and comparing living standards across countries, and it often serves as a reference point for other economic variables. Measures of real GDP, however, can be quite uncertain.

Lack of statistical capacity, mismeasurement of the economy, and the existence of informal economy, among others, can all subject real GDP measures to substantial revision. This problem becomes more acute for low and middle income countries where the data collection and compilation process is less sophisticated. Understanding the uncertainty of these measures and constructing more accurate measures are therefore of great importance to assess economic performance, facilitate cross-country comparisons, and inform policy decisions.

This paper attempts to use satellite-recorded nighttime lights to illuminate official measures of real GDP. Mostly generated by human activity, nighttime lights are visible from outer space and recorded by satellites. They have been shown to be correlated with economic activity.[1] Their global coverage makes them attractive as an alternative measure of real GDP and they are increasingly used in the economics literature. However, despite their economic relevance, nighttime lights may not have a straightforward relationship with real GDP. Meanwhile, like official measures of real GDP, they are subject to measurement errors as well, which further complicates the estimation of the functional relationship.

To illustrate such issues, Figure 1 compares satellite images of nighttime lights for mainland China, the lower 48 states of the United States, and Africa between 1992 and 2013. While all of them became brighter at night in 2013, China's transformation was most visible. Variation in nighttime lights may thus contain useful information on China's real economic growth. In contrast, the United States was already bright enough in 1992. The small change in the intensity of lights over this period may not correspond well to economic growth, most of which likely happened on the scientific and technological frontier rather than on infrastructure development. While the latter was captured by satellite, the former was certainly not. Most countries in Africa, despite their fast growth, started from low levels of income and inadequate access to electricity. As a result, they were still mostly dark in 2013 and the information contained in nighttime lights may or may not be sufficient for accurately assessing economic growth.

Figure 1 highlights that the relationship between nighttime lights and real GDP may be nonlinear, that the relative accuracy of nighttime lights to real GDP may change, and that the extent to which nighttime lights are useful as proxy for real economic activity may differ over time and across countries.

In this paper, we address the aforementioned issues by uncovering the distribution

---

[1]See, for example, Elvidge et al. [1997], Ghosh et al. [2010], Chen and Nordhaus [2011], Henderson et al. [2012], Pinkovskiy and Sala-i Martin [2016], among others.

Figure 1: Examples of Satellite Images of Nighttime Lights
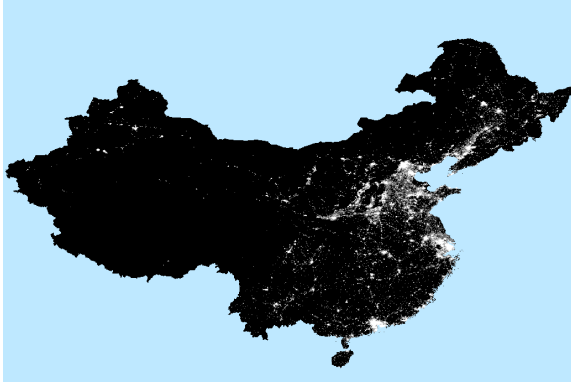
(a) China (mainland) 1992

(b) China (mainland) 2013
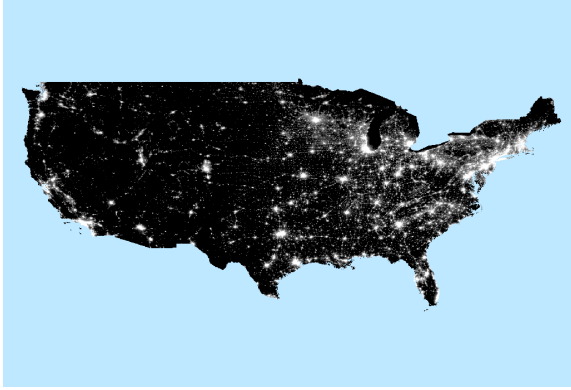
(c) United States (lower 48) 1992
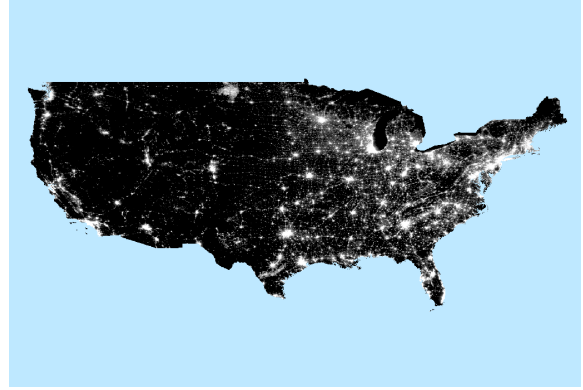
(d) United States (lower 48) 2013
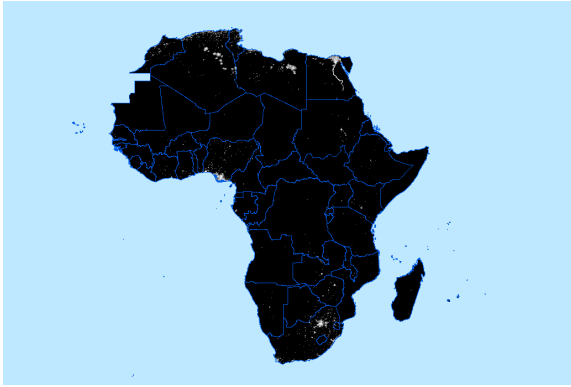
(e) Africa 1992
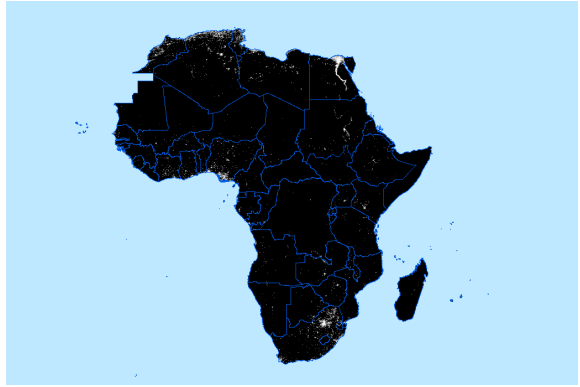
(f) Africa 2013

of measurement errors in both official GDP measures and nighttime lights as well as their functional relationship simultaneously. We provide a statistical framework based on nonclassical and nonlinear measurement error models, in which the error in official GDP per capita may depend on the country's statistical capacity and the relationship between nighttime lights and true GDP per capita can be nonlinear and vary with

geographic location. Using variation across geographic locations and different levels of statistical capacity, we establish identification of the distribution function of nighttime lights conditional on real GDP under fairly weak and reasonable statistical assumptions based on recently developed results for measurement error models.

Given our nonparametric identification results, estimates of nighttime lights' elasticity with respect to real GDP at different levels of income are naturally obtained. Such elasticities can be useful in imputing changes of economic activities in regions where official data are not available. With the estimated distributions of measurement errors, we assess the relative uncertainty of nighttime lights and real GDP and the extent to which nighttime lights can be useful to improve real GDP measures. We then construct new real GDP measures by optimally combining official measures, information in nighttime lights, statistical capacity and geographic location. We focus on two new measures. One is an optimal linear combination of official data and prediction by nighttime lights, for which we provide an estimate of the optimal weight on nighttime lights for each observation of real GDP figure. We show that this optimal linear measure performs very well across countries. The other measure is the semiparametric conditional mean that is based on the full conditional distribution of true GDP given all the observables.

To our best knowledge, this is the first paper to estimate the distribution of measurement errors in official GDP and nighttime lights directly from data. The error distributions are crucial for both understanding the uncertainty in official GDP measures and constructing more precise measures. Intuitively, we can use nighttime lights to infer the accuracy of the official GDP. This is because nighttime lights reflect real economic activities, and therefore, are correlated with the true GDP. In the meantime, nighttime lights are independent of the measurement error in the official GDP. After we identify how much nighttime lights a given amount of GDP may produce, i.e., the production function of nighttime lights, we may infer the distribution of the true GDP from the observed joint distribution of nighttime lights and the official GDP. Comparing the distribution of the true GDP with the observed distribution of the official GDP, we may pin down the signal-to-noise ratio of the official GDP. Therefore, we can provide better measures of the true GDP using additional information, such as nighttime lights.

We conduct our analysis using two nighttime lights datasets. The first one spans from 1992 to 2013 and the second from 2013 to 2017. Recorded by different satellite systems, the two datasets are not only useful in extending the analysis of nighttime lights and real GDP to more recent date, but they also serve a purpose of validating

the robustness of our identification and estimation strategy.

There are four main findings in this paper. First, the relationship between nighttime lights and real GDP is nonlinear. In our baseline specification, we estimate that the elasticity of nighttime lights with respect to real GDP per capita can be as high as 2.3 for low income countries but is close to 0 for high income countries. The elasticity steadily decreases as real GDP per capita increases, reflecting different developing mode at different stages of economic development. Intuitively, countries at early stages of development tend to build more infrastructure that generates lights at night, such as buildings and roads; countries at more advanced stages tend to focus more on technological innovation, which is less associated with lights at night.

Second, we find, perhaps not surprisingly, that measurement errors in real GDP per capita (and hence real GDP) are bigger for countries whose income is lower. There is a sharp distinction between high income countries and the rest of the countries. While high income countries have measurement errors of real GDP concentrated at zero, low and middle income countries have fat tails in the distribution of measurement errors. In other words, there is greater uncertainty in the latter countries' GDP measures and the measurement error can be substantial at times. The distinction between those with high and low statistical capacity among low and middle income countries, however, is blurred.

Third, nighttime lights are most useful for assessing and augmenting measures of real GDP in low and middle income countries. We find that the optimal weight of our new measure of real GDP on light-predicted GDP reaches 70% for middle income countries, but it declines for countries at either end of the income spectrum. For countries with extremely low levels of real GDP per capita, it is rather dark at night and as such the uncertainty in light-predicted GDP can be quite high. In contrast, for countries with high levels of real GDP per capita, nighttime lights are bright enough to reach the saturation level of satellite sensors and hence may not adequately reflect variations in economic activities. More fundamentally, limited access to electricity for low income countries and post-industrialization of high income countries are likely to disassociate their economic development from nighttime lights.

Finally, comparing our new measures with official measures of real GDP, we find that there are two types of discrepancies. First, some countries have systematically different real GDP measures than our new measures. Most notably for China, our new measure implies that annual real GDP growth is lower than official measures by 1.9 percentage points on average in the 1990s and 2000s, and 3.4 percentage points in the wake of the 2008 global financial crisis. Second, countries disrupted by conflicts

and political instability often underestimated the deterioration of the economy during downturns and its recovery afterwards. It is likely that periods of economic disruption made it difficult to track the economy accurately and the emergence of informal economy in subsequent restoration did not enter national accounts. For example, conflicts might simply disrupt tax registration of firms that would otherwise have been recorded.

The rest of the paper is organized as follows. Section 2 briefly reviews related literature. Section 3 and Section 4 describe our data and statistical framework , respectively. We present our results in Section 5. Section 6 concludes. Additional information on data is in Appendix A. Mathematical proofs of identification and asymptotic properties are provided in Appendix B. Robustness checks, including simulations and different estimates, are discussed in Appendix C.

2   Related Literature

This paper is closely related to several strands of literature.

First, we contribute to the growing literature on understanding economic growth through the lens of satellite-recorded nighttime lights. Since the seminal work of Henderson et al. [2012], nighttime lights have been increasingly used as a proxy for economic activity. For instance, Pinkovskiy and Sala-i Martin [2016] assess the relative quality of GDP per capita and survey means by comparing them to nighttime lights; Storeygard [2016] investigates the role of transport costs on the economic activity of cities proxied by nighttime lights; Alesina et al. [2016] use nighttime lights to study ethnic inequality; Henderson et al. [2018] studies the spatial distribution of economic activity proxied by nighttime lights. While most of the literature use nighttime lights directly as an alternative measure of real economic activity, we show that the relationship between nighttime lights and real GDP may differ for countries at different stages of development.

From a statistical perspective, Henderson et al. [2012] and Pinkovskiy and Sala-i Martin [2016] construct new measures of real GDP growth and real GDP per capita, respectively, through the combination of nighttime lights and official or survey-based GDP measures. While they obtain constant weights on nighttime lights, we take a step forward and show that the information content on real GDP from nighttime lights differ for each observation. For each country at each point in time, our optimal linear measure uses a different optimal weight on light-predicted GDP, and this can only be achieved when we uncover the entire distribution of measurement errors in both

6

nighttime lights and official measures of real GDP.

Second, this paper is related to the measurement error literature on identification and estimation of measurement error models. Our statistical framework is based on recently developed results for nonclassical measurement error models. Since Hu and Schennach [2008], we can generally identify and estimate nonlinear models with nonclassical measurement errors in a continuous variable. When there are only two continuous measurements for a continuous latent variable as in the current paper, nonparametric identification requires additional data information or extra restrictions. Carroll et al. [2010] use a secondary survey sample to achieve nonparametric identification, which can be interpreted as identification with two continuous measurements and two discrete instruments. Schennach and Hu [2013] impose additivity and independence to show identification is feasible with two continuous measurements only.[2] Our method relies on the latter two papers with official GDP and nighttime lights as two continuous measurements and statistical capacity and geographic location being two discrete instruments. For high income countries, our identification of error distributions relies on additivity and independence assumptions.

Third, we contribute to the literature on improving the measurement of the economy from a measurement-error perspective. Aruoba et al. [2016] improves historical United States' GDP growth at relatively high frequency and find the persistence of aggregate output dynamics to be stronger than previously thought. Feng and Hu [2013] show that the official US unemployment rate substantially underestimates the true level of unemployment. This paper aims to improve annual real GDP estimates in a measurement error model setting for low and middle income countries.

Finally, we make a contribution to the burgeoning literature on bringing satellite data to economic analysis. Donaldson and Storeygard [2016] provide a comprehensive review of applications of satellite data in economics. While many applications focus on converting satellite images to physical quantities relevant for economics, such as nighttime lights, greenness, or temperature, we focus on examining the relationship between such quantities and economic variables of interest from an econometric perspective. Our method can be applied broadly to a wide range of remote sensing data, as they inevitably contain measurement errors and their relationship with economic variables of interest may not be simple and linear. One of the benefits of our method is that we uncover the relationship without side information, which is often unavailable – the lack of alternative data sources is the very reason that satellite data are being used. Moreover, our method is based on recent results for nonlinear nonclassical

---

[2]See Hu [2017] for a short survey of the recent developments in this literature.

measurement error models, which allows flexible relationship between the latent true value and the measurement error.

3 Data and Stylized Facts

3.1 Nighttime Lights

The National Oceanic and Atmospheric Administration (NOAA) provides average-radiance cloud-free composites of nighttime lights data, which we use in this paper. As of now, there are three sets of nighttime lights data available that cover different time periods: DMSP/OLS annual composites between 1992 and 2013, VIIRS monthly composites from April 2012 onward, and VIIRS annual composites in 2015 and 2016. Annual and monthly composites were processed to different extents by scientists at NOOA. For annual composites, observations affected by sunlight, moonlight, glare, aurora, and other temporal lights have been removed. However, monthly composites have not been filtered to screen out those lights.

Figure 2: Nighttime Lights in 2010
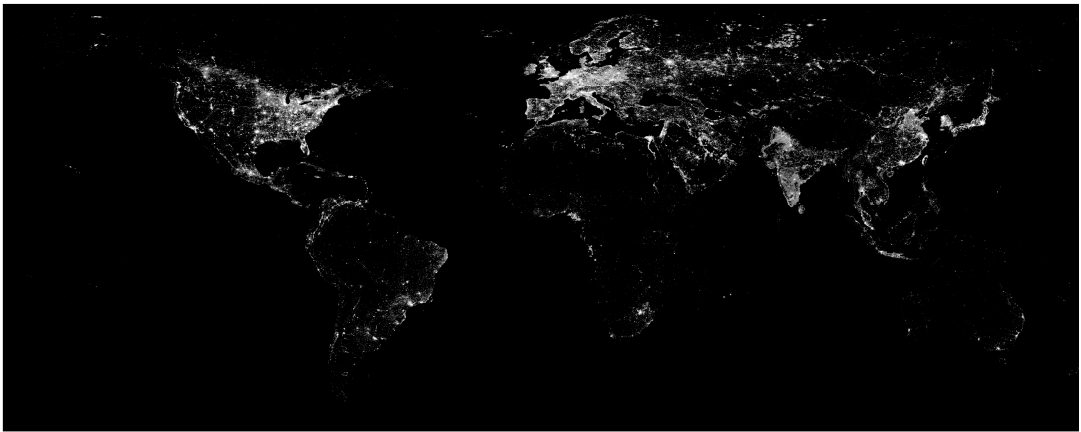
We focus primarily on DMSP/OLS data in this paper, but also extend our analysis using annual averages of VIIRS monthly composites.[3] Given the very limited sample size of VIIRS annual composites, we only use it for cross-checks. Figure 2 provides an example of the DMSP/OLS nighttime lights image in 2010.

---

[3]Unless noted otherwise, this is the data we use when we refer to VIIRS data.

To relate nighttime lights data to economic variables, such as GDP, it is important to understand the numeric pixel values of satellite images. Table 1 presents the sensor ranges of DMSP/OLS and VIIRS as well as their mapping to numeric pixel values.

Table 1: Numeric Pixel Values of Satellite Images

	DMSP/OLS	VIIRS
Radiance range (watts/cm^2/sr)	$(10^{-10}, 10^{-5})$	$(3 \times 10^{-9}, 0.02)$
Numeric value of pixels	$0, 1, \cdots, 63$	$(-1, 2 \times 10^7)$
Formula	$\frac{DN}{R} = \frac{DN_{max}}{R_{sat}}$	Radiance$\times 10^9$

Notes: DN and R are digital numbers of pixels and radiance, respectively. R_{sat} is the saturation radiance and $DN_{max} = 63$ is the maximum digital number of DMSP/OLS satellite image pixels. See, for example, Hsu et al. [2015], Shi et al. [2014].

One of the limitations of DMSP/OLS data is that it is top-coded, with the maximum pixel value corresponding to the saturation radiance of the satellite sensors. Despite such top coding, variation in nighttime lights still contain ample information on economic activities for most countries. As shown in Appendix A, while top coding might be a concern for high income city states, such as Singapore, where almost all nighttime lights reach saturation radiance, saturated pixels only account for a very small fraction of all pixels with positive values for most countries. For example, they account for less than 2.4% in the United States, 1.1% in China, and 0% in Sierra Leone.

By comparison, VIIRS has orders-of-magnitude wider radiance range and as such can be viewed as virtually not top-coded.[4] However, because VIIRS monthly composites have not been filtered to screen out temporal lights, its data can be quite noisy that background lights sometimes overwhelm artificial lights in low-lit areas.

The Database of Global Administrative Areas (known as GADM) provides administrative shape files for all countries in the world. For each country, we clip nighttime lights at each point in time to their country borders and aggregate the numeric pixel values of all pixels within their borders. We further divide the sum of nighttime lights by population and define the logarithm of total nighttime lights per capita as night light intensity, which is the variable extensively used in this paper when we refer to nighttime lights.

---

[4]For example, the brightest pixel of the United States in 2016 VIIRS annual composites has a numeric value of 4006.38 (nano watts/cm^2/sr) while the largest value the sensors can pick up is of the order of 10^7.

Appendix A provides more details on DMSP/OLS and VIIRS as well as information on statistical distributions of nighttime lights data.

3.2 GDP, Population, Statistical Capacity, and Country Location

We obtain GDP per capita (PPP, constant 2011 international dollars) and population data from the World Bank. The World Bank also provides statistical capacity ratings for low and middle income countries. While the ratings change over time, the change is small for most countries. For this reason we group countries into three categories. One category is high income countries. The other two are low and middle income countries, which we divide into those below the median of statistical capacity rating and those above. Such discretization has the additional benefit of reducing the measurement errors in statistical capacity itself.

DMSP/OLS and VIIRS satellites are polar orbiting – their orbits are perpendicular to the direction of Earth's rotation. As such a natural characterization of a country's location that could account for measurement errors in nighttime lights is its latitude. To obtain a country's latitude, we use the latitude of the centroid of its largest contiguous block.[5] Since countries differ substantially in their geographic coverage, we further discretize country locations into binary values based on whether their centroid's latitude is between the Northern and Southern Tropic or outside.[6] Such classification also takes into account the number of countries in each geographical subarea. An alternative classification is to group countries by Northern and Southern Hemisphere, but the Souther Hemisphere contains substantially fewer countries.

3.3 Summary Statistics

In total we have an unbalanced panel of 182 countries and 3870 observations based on DMSP/OLS nighttime lights data. The majority of countries have data spanning from 1992 to 2013. A similar panel is constructed for VIIRS nighttime lights data, where there are 184 countries and 920 observations. The discrepancy between the number of

---

[5]For instance, the United States has a few separate bodies of landmass, such as Alaska, Hawaii, and the lower 48 states. We use the centroid of the lower 48 states as the location of the United States. Appendix D.2 provides an illustration.

[6]Countries between the tropics generally receive more sunshine than those outside, which might affect background noise in nighttime lights. As an extreme example, the sun sets late in summer for countries closer to the arctic circle. For VIIRS monthly composites, nighttime lights are zero for Nordic countries during the summer months. While this is less concerning when we use the annual average of monthly data, differentiating measurement errors for countries at different locations can nevertheless be helpful.

countries in the two datasets arises from the availability of statistical capacity ratings.[7]
Tables 2 and 3 present the summary statistics based on nighttime lights data from
DMSP/OLS and VIIRS, respectively. As can be seen from the table, richer countries
tend to be brighter at night.

Table 2: Summary Statistics (DMSP/OLS)

Location	Statistical Capacity	Night lights per 1000 people	real GDP per capita	# of countries	# of obs
Between Tropics	Low	66	9490	12	228
Between Tropics	High	58	9680	36	786
Between Tropics	(High income)	186	40214	34	729
Outside Tropics	Low	17	5311	57	1192
Outside Tropics	High	21	6614	37	812
Outside Tropics	(High income)	78	62074	6	123
Total	-	63	15097	182	3870

Table 3: Summary Statistics (VIIRS)

Location	Statistical Capacity	Night lights per 1000 people	real GDP per capita	# of countries	# of obs
Between Tropics	Low	101	9250	10	50
Between Tropics	High	63	12074	30	150
Between Tropics	(High income)	172	40720	45	225
Outside Tropics	Low	28	5169	51	255
Outside Tropics	High	24	8881	35	175
Outside Tropics	(High income)	81	46064	13	65
Total	-	76	18807	184	920

3.4 Stylized Facts

3.4.1 Correlations

Nighttime lights directly reflects some economic activities at night, such as traffic
flows, nearly all types of consumption, and factories working around the clock. It also
reflects less productive activities, such as lights from street lamps and skyscrapers.
Obviously, the relationship between nighttime lights and economic activity is complex.
We abstract from exact channels through which economic activities produce lights at

---

[7]The two countries are Barbados and the Czech Republic.

night. Instead, our use of nighttime lights as a measure of true GDP is predicated on the high correlation between them.

Table 4 presents the correlations between real GDP per capita and night light intensity for the three sets of nighttime lights data currently available. The overall correlation is very high (> 0.85) for annual composites of both DMSP/OLS and VI-IRS data and slightly less (0.66) for annual averages of VIIRS monthly composites. The correlation is decreasing in general as countries' income level rises. VIIRS annual composites are ideal data for revealing the correlations because background noise has been removed and there is essentially no top-coding. Notably, by comparison, top coding in DMSP/OLS annual composites makes the correlation for high income countries weaker,[8] while background noise in VIIRS monthly composites makes it negative for low income countries.[9]

Table 4: Correlation between GDP per capita and Night Light Intensity

	DMSP/OLS 1992-2013 (A)	VIIRS 2015-2016 (A)	VIIRS 2013-2017 (M)
Low income	0.70	0.47	-0.02
Lower middle income	0.66	0.42	0.29
Upper middle income	0.40	0.50	0.42
High income	0.09	0.20	0.15
All countries	0.85	0.87	0.66

Notes: In parentheses, A indicates annual data and M annual average of monthly data. Variables are in logarithms.

3.4.2 Nonlinearity

As shown in Table 4, the fact that the correlation between nighttime lights and GDP is decreasing with income levels suggests that their relationship could be nonlinear. Figure 3 contrasts night light intensity and real GDP per capita graphically. The non-linearity is visible in annual data. For annual averages of VIIRS monthly composites, it is noticeable that night light intensity is noisy at low levels of real GDP per capita as a result of background noise.

---

[8]Another contributing factor is the overpass time of the satellites. While DMSP/OLS's overpass time is between 7-9pm local time, that of VIIRS is after midnight. See Appendix A for more details.

[9]The negative correlation arises mainly because of a few countries with very low GDP per capita, where background noise overwhelms artificial lights. For example, excluding the Central African Republic, which has the lowest GDP per capita in the sample, the overall correlation is 0.12.

Figure 3: Nighttime Lights vs. GDP (1992-2017)

(a) DMSP/OLS 1992-2013   (b) VIIRS 2013-2017
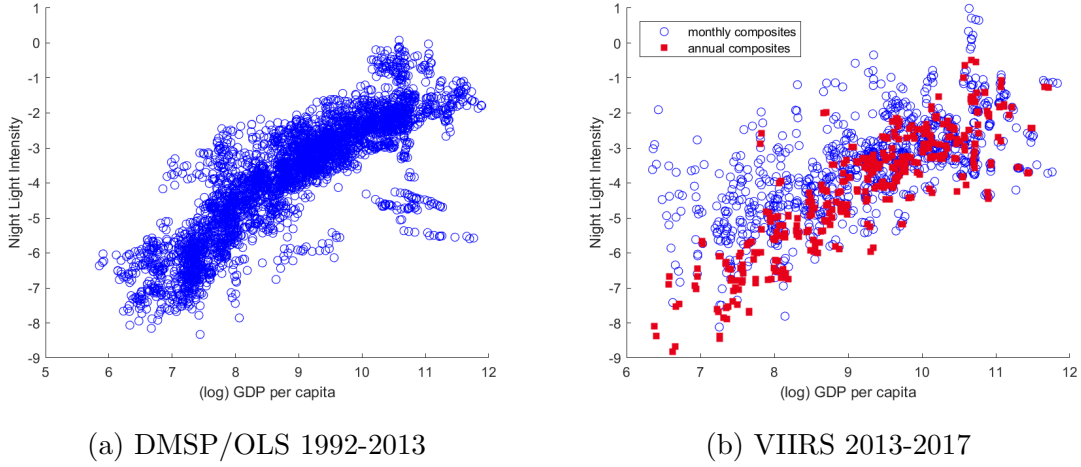
Notes: Each dot/square represents a country-year observation. On right, blue dots are annual averages of VIIRS monthly composites.

Before delving into our statistical framework, it is useful to examine the data with some simple regressions. Table 5 presents the results from ordinary least squares regressions of night light intensity on real GDP per capita with and without fixed effects. For DMSP/OLS data (columns (1) and (2)), the statistical significance of the second order term of GDP indicates that the relationship between night light intensity and real GDP per capita is nonlinear. The nonlinearity holds with and without country and year fixed effects, which suggests that as a country becomes richer, the elasticity of night light intensity with respect to real GDP per capita decreases, a point that we will confirm in our formal statistical framework.

For VIIRS annual composites, column (3) suggests that the relationship is also nonlinear. Note that VIIRS annual composites are not top-coded. The nonlinearity therefore does not come from concavity imposed by top coding, which might be a concern for DMSP/OLS data. Column (4) shows that such nonlinearity is driven by country fixed effects. Not surprisingly, with only two years of observations for VIIRS annual composites, variations in nighttime lights almost entirely come from discrepancies between countries rather than within countries. From column (1) to (4), R^2 is high (> 0.75) without fixed effects and very high (> 0.98) with fixed effects. This implies that night lights are useful for cross-country comparisons while fixed effects are important to account for some level shifts, i.e., countries might differ systematically in their habits of using lights at night.

For annual averages of VIIRS monthly composites, the relatively low R^2 in column (5) stems directly from the contamination of background light noise of a few low income

13

Table 5: Nonlinear Relationship between Night Light Intensity and GDP per capita

	DMSP/OLS 1992-2013 (A)		VIIRS 2015-2016 (A)		VIIRS 2013-2017 (M)	
	(1)	(2)	(3)	(4)	(5)	(6)
	Night Light Intensity					
(log) GDP per capita	4.163***	1.956***	3.974***	2.654	0.721*	5.136***
	(0.143)	(0.137)	(0.505)	(2.110)	(0.398)	(1.517)
(log) GDP per capita squared	-0.171***	-0.0928***	-0.151***	-0.0958	0.00155	-0.254***
	(0.00800)	(0.00780)	(0.0277)	(0.115)	(0.0218)	(0.0822)
country FE	-	Yes	-	Yes	-	Yes
year FE	-	Yes	-	Yes	-	Yes
Obs	3870	3870	367	366	920	920
Adjusted R^2	0.751	0.983	0.771	0.998	0.431	0.950

Notes: FE is fixed effects. Standard errors are in parentheses. $^*p < 0.10$, $^{**}p < 0.05$, $^{***}p < 0.01$. Clustered standard errors (not shown in the table) at the country level do not change the level of significance of the second order term of GDP in any of the above regressions.

countries. Controlling for fixed effects, the nonlinearity is visible.

Taken together, there is strong evidence that the relationship between night light intensity and real GDP per capita is nonlinear. The nonlinearity exists both between and within countries – the latter only emerges with enough time span for a country's income level to rise substantially.

4 Statistical Framework

In this section, we present a statistical framework to analyze the nighttime lights data in relation to GDP. Under fairly weak assumptions, the nonlinear relationship between nighttime lights and GDP and the distribution of measurement errors in each of them are identified. Elasticities of nighttime lights with respect to GDP per capita are naturally obtained. We then construct a more accurate and robust measure of GDP per capita by optimally combining national accounts data and prediction by nighttime lights.

4.1 Baseline Setup

Let $y_{i,t}^*$ denote the true real GDP per capita in logarithm for country i in year t. It is measured as $y_{i,t}$ with error. Let $s_{i,t}$ stand for the statistical capacity of country i at time t. Let $z_{i,t}$ denote nighttime lights per capita in logarithm. It is related to the true real GDP per capita but also contains measurement error. Let l_i stand for the latitude of the country.

Our baseline specification assumes that official GDP contains an additive measurement error, whose distribution varies with statistical capacity,

$$y_{i,t} = y_{i,t}^* + \epsilon_{i,t}^y(s_i). \tag{1}$$

Meanwhile, nighttime lights are related to the true latent GDP through an unknown production function $m(\cdot)$ and an additive error term that differ by geographic location,

$$z_{i,t} = m(y_{i,t}^*) + \epsilon_{i,t}^z(l_i) \tag{2}$$

The additive nature of measurement errors are not necessary for identification, but are assumed for the purpose of estimation.

The specification of the production function $m(\cdot)$ is informed by the data. As suggested by Figure 3, a quadratic function form is sufficient.[10] The distributions of the error terms $\epsilon_{i,t}^y$ and $\epsilon_{i,t}^z$ are allowed to be nonparametric.

A Heuristic Example

A special case of Equations (1) and (2) is when the night light production function is linear and error distributions are the same for all countries:

$$\begin{aligned} y_{i,t} &= y_{i,t}^* + \epsilon_{i,t}^y, \\ z_{i,t} &= \beta y_{i,t}^* + \epsilon_{i,t}^z. \end{aligned} \tag{3}$$

Under the assumption that measurement errors are classical, β cannot be identified from second moments. To see this, we take variances and covariances of the above equations,

$$\begin{aligned} \text{var}(y) &= \text{var}(y^*) + \text{var}(\epsilon^y), \\ \text{var}(z) &= \beta^2 \text{var}(y^*) + \text{var}(\epsilon^z), \\ \text{cov}(y, z) &= \beta \text{var}(y^*). \end{aligned}$$

Because there are only three equations but four unknowns ($\text{var}(\epsilon^y)$, $\text{var}(\epsilon^z)$, $\text{var}(y^*)$, and β), the system cannot be identified. The literature has dealt with identification in this case by either assuming additional relationship between $\text{var}(\epsilon^y)$ and $\text{var}(\epsilon^z)$ (Henderson et al. [2012]) or adding auxiliary data (Pinkovskiy and Sala-i Martin [2016]).

In fact, Schennach and Hu [2013] shows that the system (3) can be identified with higher moments. In other words, β and the distributions of y^*, ϵ^y and ϵ^z can be uniquely estimated from the joint distribution of y and z.

---

[10]We consider higher order polynomials in the Appendix.

In our baseline specification (equations (1) and (2)), we relax the assumptions in the linear special case (3) substantially. First, we allow the night light production function to be nonlinear, which is suggested by evidence in Section 3.4.2. Second, we allow the error terms to vary with a country's statistical capacity and location, which is more realistic.

4.2 Nonparametric Identification

We obtain nonparametric identification in a more general setting than our baseline specification, where the error terms need not be additive.

Let $f(\cdot|\cdot)$ be a generic conditional probability density function. We make the following assumptions.

Assumption 1

$$f(z_{i,t}|y_{i,t}^*, y_{i,t}, s_i, l_i) = f(z_{i,t}|y_{i,t}^*, l_i). \tag{4}$$

This assumption implies that the nighttime lights are related to the true real GDP per capita and the geographic location of a country, but have nothing to do with how its GDP is measured or its statistical capacity.

Assumption 2

$$f(y_{i,t}|y_{i,t}^*, s_i, l_i) = f(y_{i,t}|y_{i,t}^*, s_i). \tag{5}$$

This assumption implies that statistical capacity captures how accurate GDP is measured regardless of the location of the country.

With economic Assumptions 1 and 2 and four additional technical assumptions in Appendix B.1, we have the following nonparametric identification result:

Theorem 1 *Suppose Assumptions 1–6 hold. Then, the distribution function $f(z, y, s, l)$ uniquely determines the joint distribution function $f(z, y, y^*, s, l)$ satisfying*

$$f(z, y, y^*, s, l) = f(z|y^*, l)f(y|y^*, s)f(y^*, s, l). \tag{6}$$

Proof: See Appendix B.2.

This theorem presents a set of sufficient conditions under which all the distributions containing the latent true GDP can be uniquely determined by the observed joint distribution of GDP and nighttime lights from countries with different statistical capacity and at different locations:

$$
\begin{aligned}
f(z_{i,t}, y_{i,t}, s_i, l_i) &= \int f(z_{i,t}, y_{i,t}, y_{i,t}^*, s_i, l_i) dy^* \\
&= \int f(z_{i,t}|y_{i,t}^*, l_i) f(y_{i,t}|y_{i,t}^*, s_i) f(y_{i,t}^*, s_i, l_i) dy_{i,t}^*
\end{aligned}
$$

Such a nonparametric identification result implies that consistent estimation is possible for parametric, semiparametric, or nonparametric specifications. In order to focus on the relationship between the nighttime lights and the latent true GDP and also to take the sample size into account, we adopt the baseline specification to simplify the measurement error structure.

4.3   Sieve Maximum Likelihood Estimation

Given the general nonparametric identification, we provide a semiparametric estimator as suggested in Carroll et al. [2010]. We develop our estimator based on an i.i.d sample, which can be extended to account for covariates and time series data. We assume that there is a random sample $\{z_i, y_i, s_i, l_i\}_{i=1}^n$.

The specification of the production function $m(\cdot)$ is informed by the data (Figure 3) and assumed to be a quadratic function. The error terms $\epsilon_{i,t}^y$ and $\epsilon_{i,t}^z$ are allowed to have a general density function. Therefore, in this empirical study, we adopt a parametric specification of function $m(\cdot; \theta)$ and leave other elements nonparametrically specified in the baseline specification in equations (1) and (2). Let the true value of the unknowns be $\alpha_0 \equiv (\theta_0^T, f_{y^*|s,l}, f_{\epsilon^y|s}, f_{\epsilon^z|l})^T$, where $f_{A|B}$ denotes the distribution of A conditional on B. We then introduce a sieve MLE estimator $\widehat{\alpha}$ for α_0, and establish the asymptotic normality of $\widehat{\theta}$. These results can also be extended to the case where the function m is misspecified.

In the sieve MLE estimator, we use finite dimensional parametric representations to approximate the nonparametric densities in α_0, where the dimension may increase with the sample size. Let $\mathcal{A}$ be the parameter space. The log-joint likelihood for $\alpha \equiv (\theta^T, f_1, f_2, f_3)^T \in \mathcal{A}$ is given by:

$$\sum_{i=1}^n \log f(z_i, y_i, s_i, l_i) \;\; = \;\; \sum_{i=1}^n \ell(D_i; \alpha),$$

in which $D_i = (z_i, y_i, s_i, l_i)$ and

$$
\begin{aligned}
\ell(D_i; \alpha) \;\; &\equiv \;\; \ell(z_i, y_i, s_i, l_i; \theta, f_1, f_2, f_3) \\
&= \;\; \log\{ \int f_1(y^*|s_i, l_i) f_2(y_i - y^*|s_i) f_3(z_i - m(y^*; \theta)|l_i) dy^* \} + \log f(s_i, l_i).
\end{aligned}
$$

Let $E[\cdot]$ denote the expectation with respect to the underlying true data generating process for D_i. Then

$$\alpha_0 = \arg \sup_{\alpha \in \mathcal{A}} E\left[\ell(D_i; \alpha)\right].$$

We then use a sequence of finite-dimentional sieve spaces $\mathcal{A}_n$ to approximate the functional space $\mathcal{A}$. The semiparametric sieve MLE $\widehat{\alpha}_n \in \mathcal{A}$ is defined as:

$$\widehat{\alpha}_n = \arg\max_{\alpha \in \mathcal{A}_n} \sum_{i=1}^{n} \ell(D_i; \alpha).$$

Under assumptions presented in Appendix B.4, we show the consistency of estimator $\widehat{\alpha}_n$ for α_0 and the convergence rate of the nonparametric components. Furthermore, we show in Appendix B.5 that the sieve MLE $\widehat{\theta}_n$ is asymptotically normally distributed around the true value θ_0. When the parametric model $E[z|y^*, l] = m(y^*; \theta)$ is misspecified, the estimator $\widehat{\theta}_n$ is still asymptotically normally distributed, but around a pseudo true value. In fact, the estimator $\widehat{\theta}_n$ is semiparametrically efficient for θ_0.

4.4 Constructing Better Measures of GDP

With the conditional distribution of nighttime lights and official real GDP per capita at hand, we construct new and more accurate measures of real GDP per capita that optimally combine the information in these two measures.

First, we estimate the optimal linear combination of official data and prediction by nighttime lights. As a convex combination of two GDP measures, it is very robust across countries.

We then take a step further and provide a measure based on the semiparametric conditional mean, which makes full use of the observed information through conditional distributions. However, it requires more data so that it may not be robust in the area where observations are sparse.

4.4.1 Optimal Linear Measure

The optimal linear measure is based on a linear combination of official real GDP per capita and prediction by nighttime lights:

$$\hat{y^*}_{i,t} = \lambda_{i,t} \hat{y}_{i,t} + (1 - \lambda_{i,t}) y_{i,t}, \tag{7}$$

where $\hat{y}_{i,t}$ is nighttime light-predicted GDP per capita, $y_{i,t}$ is official GDP per capita, and $\lambda_{i,t}$ is the weight.

Obtaining prediction by nighttime lights is necessary for converting night light intensity into measures of real GDP per capita. The weight $\lambda_{i,t}$ determines the extent to which the new GDP measure depends on the prediction by nighttime lights.

Crucially, to obtain the optimal weight $\lambda_{i,t}^*$, we need information on measurement errors in both $\hat{y}_{i,t}$ and $y_{i,t}$, which in turn rely on distributions of measurement errors

in nighttime lights and official GDP per capita identified previously.

Prediction by Nighttime Lights

We regress official real GDP per capita on nighttime lights with country and year fixed effects,

$$y_{i,t} = \beta_1 z_{i,t} + \beta_2 z_{i,t}^2 + \delta_i D_i^c + \gamma_t D_t^y + \eta_{i,t}, \tag{8}$$

where D^c and D^y are country and year dummies, respectively. The nighttime light-predicted real GDP per capita is defined as

$$\hat{y}_{i,t} = \hat{\beta}_1 z_{i,t} + \hat{\beta}_2 z_{i,t}^2 + \hat{\delta}_i D_i^c + \hat{\gamma}_t D_t^y. \tag{9}$$

The predictive model in equation (9), despite its parsimony, takes several important factors into account. The second order term is intended to capture the nonlinearity between night light intensity and real GDP per capita. Country fixed effects allow for countries' different habits of using lights at night. Year fixed effects take account of factors such as satellite sensor decay over time.

Optimal Linear Combination

To obtain the optimal linear combination, we minimize the conditional mean squared error of our new measure, i.e.,

$$\lambda_{i,t} = \arg\min_{\lambda} E\left[(\hat{y^*}_{i,t} - y_{i,t}^*)^2 | z_{i,t}, s_i, l_i\right], \tag{10}$$

where $y_{i,t}^*$ is the true GDP. By equations (1) and (2), this conditional mean squared error can be decomposed into two parts:

$$E\left[(\hat{y^*}_{i,t} - y_{i,t}^*)^2 | z_{i,t}, s_i, l_i\right]$$
$$= E\left[(\lambda(\hat{y}_{i,t} - y_{i,t}^*) + (1-\lambda)(y_{i,t} - y_{i,t}^*))^2 | z_{i,t}, s_i, l_i\right]$$
$$= \lambda^2 E\left[(\hat{y}_{i,t} - y_{i,t}^*)^2 | z_{i,t}, s_i, l_i\right] + (1-\lambda)^2 E\left[(\epsilon^y)^2 | s_i\right]. \tag{11}$$

The first term in equation (11) captures the uncertainty in nighttime light-predicted GDP per capita,[11] whereas the second term captures the uncertainty in official GDP per capita.

---

[11]Note that

$$E\left[(\hat{y}_{i,t} - y_{i,t}^*)^2 | z_{i,t}, s_{i,t}, l_i\right] = \frac{\int (\hat{y}(z_{i,t}) - y_{i,t}^*)^2 f_{\epsilon^z}(z_{i,t} - m(y^*)) f(y^*|s_i, l_i) \, dy^*}{\int f_{\epsilon^z}(z_{i,t} - m(y^*)) f(y^*|s_i, l_i) \, dy^*}$$

is a function of $z_{i,t}$. And we treat the country and year dummies as exogenous variables given $(z_{i,t}, s_{i,t}, l_i)$.

The optimal weight then depends on the relative uncertainty in these two measures of GDP per capita and equals,

$$\lambda_{i,t} = \frac{E\left[(\epsilon^y)^2 \,|s_i\right]}{E\left[\left(\hat{y}_{i,t} - y_{i,t}^*\right)^2 |z_{i,t}, s_i, l_i\right] + E\left[(\epsilon^y)^2 \,|s_i\right]}. \tag{12}$$

Notice that $\lambda_{i,t}$ is always in $[0, 1]$, which makes the optimal linear measure always between official GDP per capita and prediction by nighttime lights. In addition, $\lambda_{i,t}$ is country and time dependent.

4.4.2 Semiparametric Conditional Mean

Given that we have identified the distribution of the true GDP joint with all the observables in the semiparametric specification, a natural measure of the true GDP is the conditional mean of the distribution, i.e., $E[y_{i,t}^*|y_{i,t}, z_{i,t}, s_{i,t}, l_i]$. Notice that the conditional mean may also be considered as a minimizer of the mean squared error conditional on all the observables, particularly including $y_{i,t}$, which makes it different from the previous optimal linear measure. Under our nonparametric identification and semiparametric specification, it follows that

$$E[y_{i,t}^*|y_{i,t}, z_{i,t}, s_i, l_i] = \frac{\int y^* f(y^*|s_i, l_i) f(y_{i,t} - y^*|s_i) f(z_{i,t} - m(y^*; \theta)|l_i) dy^*}{\int f(y^*|s_i, l_i) f(y_{i,t} - y^*|s_i) f(z_{i,t} - m(y^*; \theta)|l_i) dy^*}.$$

Compared to the optimal linear measure, while the the semiparametric conditional mean $E[y_{i,t}^*|y_{i,t}, z_{i,t}, s_i, l_i]$ has the clear advantage of making full use of the information in the conditional distributions, its nonparametric feature makes it less robust than the previous optimal linear measure because it requires a large sample size to perform well. In the sparse area of the empirical distribution of $(y_{i,t}, z_{i,t}, s_i, l_i)$, the semiparametric conditional mean can be volatile, whereas the optimal linear measure remains robust; in the area where the density $f(y_{i,t}^*|y_{i,t}, z_{i,t}, s_i, l_i)$ takes a relatively larger value, it is stable and close to the optimal linear measure. This implies, for example, for extremely low or high income countries where observations are few, it is likely to be quite off, and for middle income countries, it is close to the optimal linear measure. For this reason, we make the optimal linear measure our choice of new measure for the true real GDP per capita.

5 Results

5.1 Nighttime Lights' Elasticity of Real GDP per capita

Table 6 displays the estimated nighttime light production function for DMSP/OLS data. The estimates are quite precise with each parameter statistically significant at the 0.01 level. Notably, the parameter estimate on the quadratic term is non-zero, confirming the nonlinear relationship indicated in Section 3.4.2.

Table 6: Estimated Light Production Function (DMSP/OLS)

$m(y^*) = \theta_0 + \theta_1 y^* + \theta_2 (y^*)^2$			
Parameter	θ_0	θ_1	θ_2
Point Estimate	0.398	1.234	-0.244
Standard Error	(0.176)	(0.139)	(0.049)

Notes: Standard errors are based on 400 sample bootstraps. Night light intensity and log real GDP per capita are re-centered at zero for estimation. The center corresponds to real GDP per capita of $7,503 (2011 international dollars).

With a quadratic light production function $m(y^*) = \theta_0 + \theta_1 y^* + \theta_2 (y^*)^2$, the elasticity of night light intensity with respect to real GDP per capita can be conveniently calculated as its derivative, $\theta_1 + \theta_2 y^*$.[12] Table 7 presents point estimates of a set of elasticities at various income levels. Most low income countries have elasticities around 2 whereas most high income countries have elasticities below 0.5. For countries or subnational regions where GDP information is not available, these elasticities can be useful to impute GDP from nighttime lights.

Table 7: Nighttime Lights' Elasticities (DMSP/OLS)

Real GDP per capita	500	1,000	2,000	3,000	5,000	10,000	20,000	30,000	50,000
Night Light Elasticity	2.34	2.04	1.74	1.56	1.34	1.04	0.74	0.56	0.34

Notes: Real GDP per capita is in 2011 international dollars.

Table 8 presents the results for VIIRS data. The estimates are much less precise due to the limited number of observations. In particular, the quadratic term is not

---

[12]For the purpose of estimation, we have re-centered the GDP data at zero. As such the elasticity of real GDP per capita follows $\theta_1 + \theta_2(y^* - \log(7503))$, where y^* is the logarithm of real GDP per capita in 2011 international dollars.

statistically significant for the full sample. This is mainly driven by a few countries with extremely low income whose background noise overwhelms nighttime lights, as shown in the comparison between monthly and annual composites in Figure 3b. In fact, if we exclude five countries with lowest average income between 2013-2017, the quadratic term turns statistically significant.[13] The elasticity of VIIRS night light intensity with respect to real GDP per capita, if one ignores the quadratic term, is close to unity. With the quadratic term, Table 9 presents point estimates of elasticities. There is considerable uncertainty in these estimates because of the sample size. Notably, excluding the five countries, elasticity estimates become higher for low income countries and lower for high income countries.

Table 8: Estimated Light Production Function (VIIRS)

$m(y^*) = \theta_0 + \theta_1 y^* + \theta_2(y^*)^2$			
Parameter	θ_0	θ_1	θ_2
Point Estimate	0.267	0.959	-0.164
Standard Error	(0.170)	(0.248)	(0.157)
Excl. 5 countries with lowest income			
Point Estimate	0.347	0.832	-0.349
Standard Error	(0.182)	(0.277)	(0.173)

Notes: Standard errors are based on 400 sample bootstraps. Night light intensity and log real GDP per capita are re-centered at zero for estimation. The center corresponds to real GDP per capita of $10,365 (2011 international dollars). Excluding 5 low income countries, (the Central African Republic, Burundi, Congo, Niger, and Liberia), the center corresponds to real GDP per capita of $11,145.

Table 9: Nighttime Lights' Elasticities (VIIRS)

Real GDP per capita	1,500	2,000	3,000	5,000	10,000	20,000	30,000
Night Light Elasticity	1.59	1.50	1.37	1.20	0.97	0.75	0.61
Excl. 5 countries with lowest income							
Night Light Elasticity	2.23	2.03	1.75	1.39	0.91	0.43	0.14

Notes: Real GDP per capita is in 2011 international dollars.

---

[13]The five countries are the Central African Republic, Burundi, Congo, Niger, and Liberia.

Figure 4: Estimation Results with Quadratic Light Production Function

(a) DMSP/OLS   (b) VIIRS
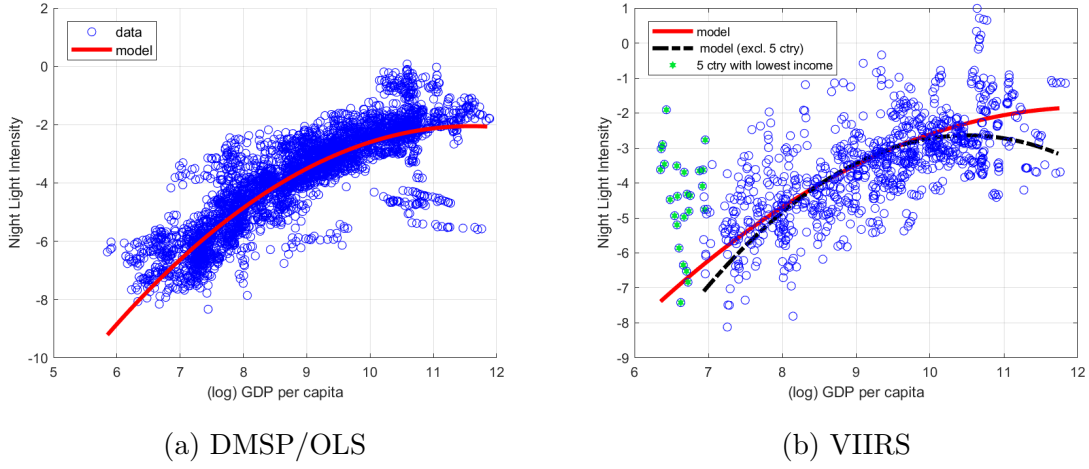
    With an abuse of notation, Figure 4 superimpose the estimated light production functions on the data. Because each graph's horizontal axis corresponds to true GDP per capita for the model but official GDP per capita with measurement errors for the data, they are not directly comparable. Nevertheless, the two graphs show similar evidence of nonlinearity in the relationship between real GDP per capita and night light intensity.

5.2   Uncertainty in Real GDP per capita

Figure 5 compares the probability density function of measurement errors of real GDP per capita for three groups of countries: high income, high statistical capacity, and low statistical capacity. The latter two groups contain only low and middle income countries.

    There is a sharp distinction between high income countries and the rest. Measurement errors of high income countries' real GDP per capita are concentrated at zero, indicating relatively high precision in official figures. In contrast, low and middle income countries' distribution of measurement errors have fat tails, suggesting that measurement errors are generally of bigger size. Among low and middle income countries, both DMSP/OLS and VIIRS data suggest that those with high statistical capacity tend to have similar measurement errors to those with low statistical capacity.

5.3   New Measures of Real GDP per capita

We focus on the optimal linear measure of real GDP per capita presented in equation (7), which depends on nighttime light-predicted real GDP per capita, official GDP per

Figure 5: Distribution of Measurement Errors of Real GDP per capita

(a) DMSP/OLS

(b) VIIRS
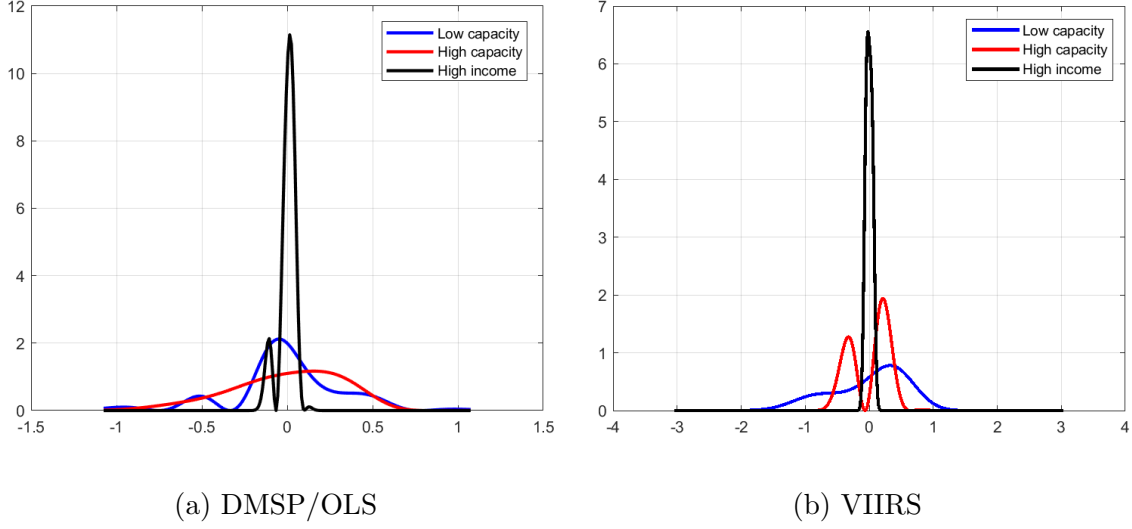
Notes: Of low and middle income countries, high capacity and low capacity refer to those above and below the median of statistical capacity, respectively. The spikes in the estimated probability density functions result from the choice of base functions used to approximate the distributions of measurement errors. As the sample size increases, these spikes will typically be smoothed out.

capita, as well as the optimal weights to combine them.

The high correlations between night light intensity and GDP per capita, as indicated in Table 4, imply that prediction by night lights (equation (9)) would in general be close to official GDP per capita. Table 10 compares the mean squared error of regression (8) between countries with different income status. The mean squared error of light-predicted GDP per capita for low income countries is almost twice as large as high income countries. In other words, there is greater discrepancy between light-predicted GDP per capita and official figures for low income countries.

Table 10: Mean Squared Error by Income Status

World Bank Country Classification	Low Income	Lower Middle Income	Upper Middle Income	High Income
Mean squared error	0.02	0.02	0.07	0.01
# observations	1212	1121	673	852

Notes: This table compares the MSE of the regression $y_{i,t} = \beta_1 z_{i,t} + \beta_2 z_{i,t}^2 + \delta_i D_i^c + \gamma_t D_t^y + \eta_{i,t}$ for countries of different income groups.

The optimal weights are calculated according to equation (12). Figure 6 contrasts

the optimal weights against real GDP per capita based on DMSP/OLS data.[14] There is broadly a bell-shaped pattern. Countries with very low or high income tend to have small weights on prediction by nighttime lights, whereas countries in the middle of the income spectrum have comparatively high weights.

Figure 6: Optimal Weights and Real GDP per capita: DMSP/OLS 1992-2013
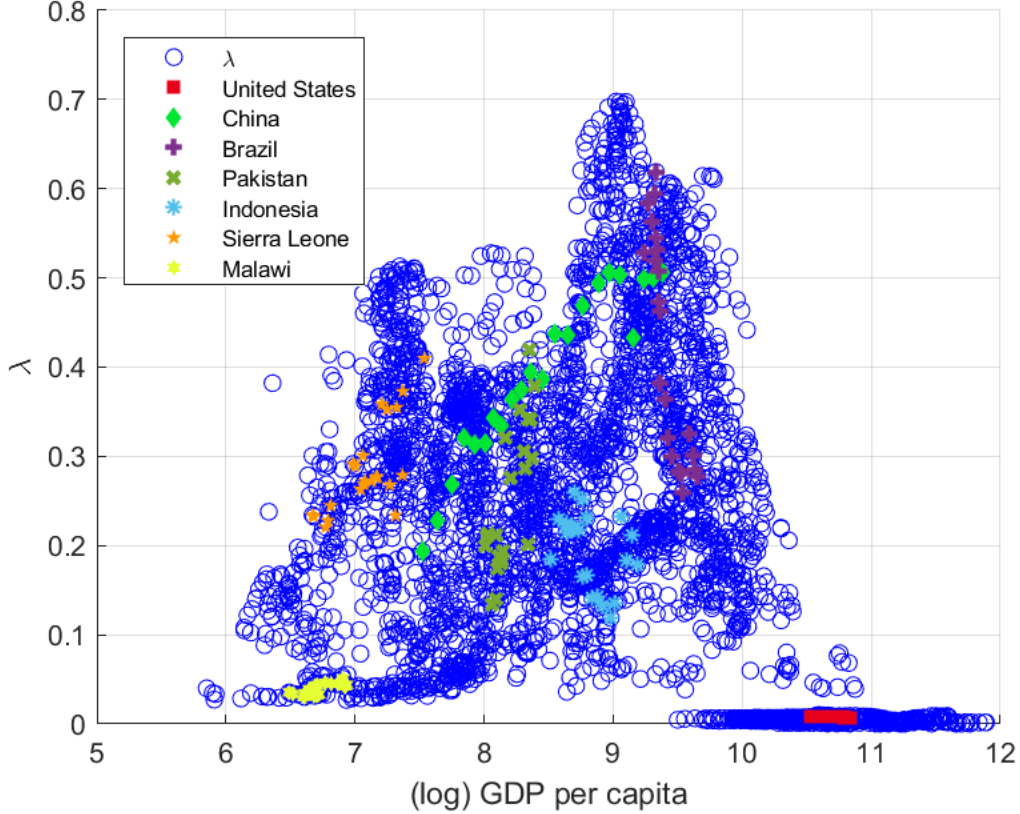
The optimal weight makes use of the relative accuracy of nighttime light-predicted GDP and official GDP figures. Intuitively, for countries with extremely low levels of real GDP per capita, it is rather dark at night and as such the uncertainty in nighttime light-predicted GDP can be quite high. For example, night light intensity for Malawi is almost zero as a result of paltry access to electricity in the country. Our optimal weights on nighttime light-predicted GDP are below 0.05 for Malawi. In contrast, high income countries tend to have the most accurate national accounts data. It is therefore not surprising that we also obtain almost zero weights for high income countries such as the United States.

Nighttime lights can play a big role in improving real GDP per capita measures for the majority of middle and low income countries. Figure 6 shows that for fragile states

---

[14]Optimal weights based on VIIRS data display a similar pattern.

like Sierra Leone, emerging markets such as China, Brazil, Indonesia, and Pakistan, our optimal weights on nighttime light-predicted GDP range from 0.2 to 0.6.

5.4 Official vs. New Measures

5.4.1 Two Types of Discrepancy

Examination of official measures of real GDP per capita and our new measures for every country in our data sets reveals that there are broadly two types of discrepancy.

The first type is systemic discrepancy. For example, panel (a) of Figure 7 shows that based on the optimal linear measure, the Chinese economy was growing at a slower rate than suggested by official figures over the past decades, but particularly so after 2005. Panel (b) shows that India under the optimal linear measure also grew less faster than official figures suggested, though the difference is much smaller compared to China. Panel (c) and (d) show that for Brazil and South Africa, the optimal linear measure implies slightly higher real GDP per capita in recent years.

While we focus on real GDP per capita previously, we can obtain real GDP growth estimates by removing population from real GDP per capita. Concretely, let g_t and p_t be real GDP growth and population growth, respectively, then $g_t = g_t^y + p_t$, where $g_t^y = y_t - y_{t-1}$ is real GDP per capita growth. Since demographics is deterministic and population estimates are relatively accurate, most of the measurement errors in real official GDP per capita figures can be attributed to real GDP.

Table 11 compares real GDP growth for China, India, Brazil, and South Africa from 1992 to 2017. Our new measure suggests that China's real GDP growth has been consistently lower than official figures. In particular, our new measure implies that annual real GDP growth is lower than official measures by 1.9 percentage points on average in the 1990s and 2000s, 3.4 percentage points in the wake of the 2008 global financial crisis, and 1.5 percentage points more recently. We discuss more about China's real GDP growth in the next section.

The second type is the discrepancy for conflict-torn economies, which stems from periods of economic disruption and restoration. Countries disrupted by conflicts and political instability often underestimated the deterioration of the economy during downturns and its recovery afterwards. For example, Figure 8 contrasts the optimal linear measure against official measure for the Democratic Republic of the Congo, Djibouti, Kenya, and Sierra Leone, respectively.

The Democratic Republic of the Congo was in a state of conflict until 2001 when UN peacekeepers arrived. When its economic situation deteriorated between 1992-

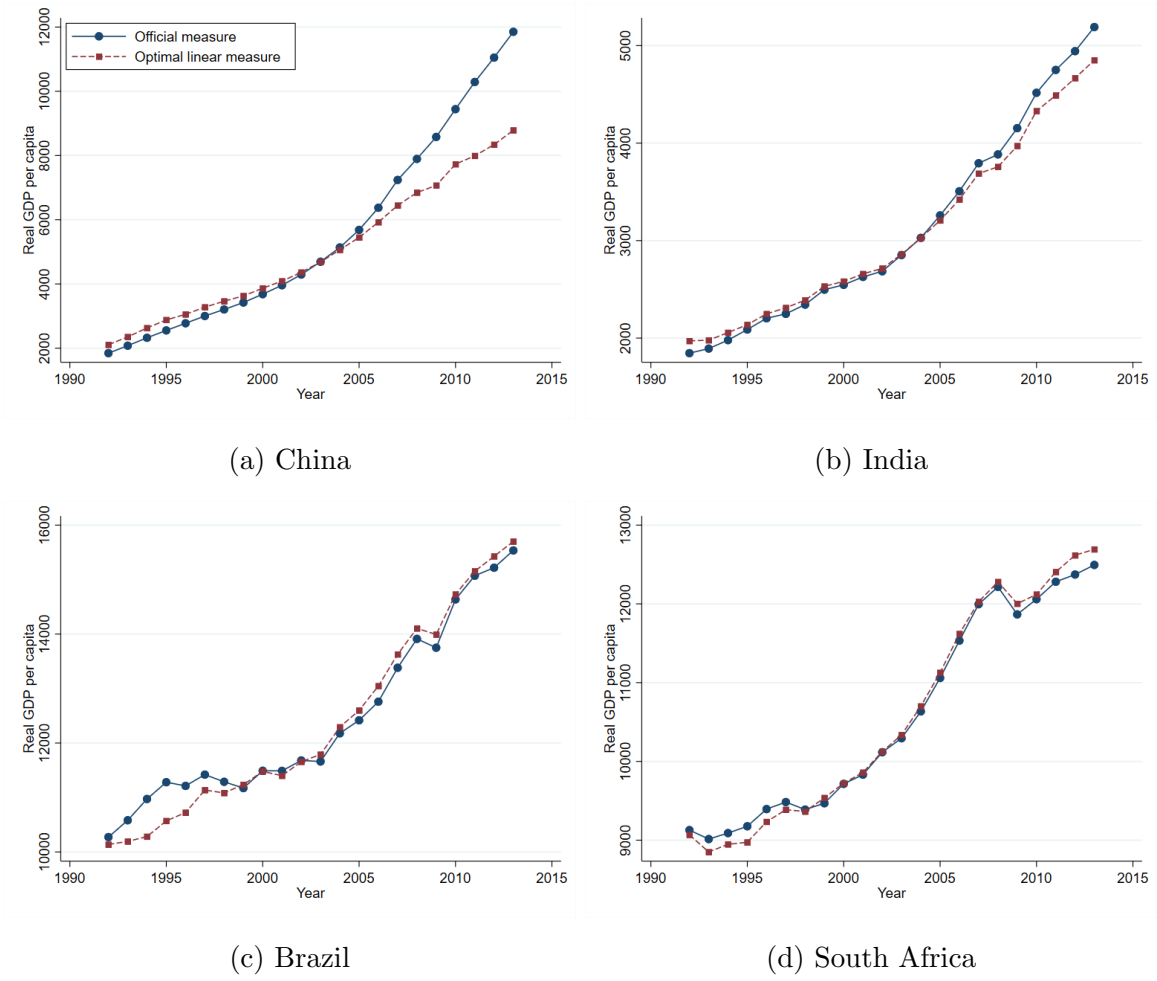Figure 7: Real GDP per capita: Selected Emerging Markets

(a) China

(b) India

(c) Brazil

(d) South Africa

Table 11: Real Economic Growth: Selected Emerging Markets

Real GDP Growth	1992-2008		2009-2013		2014-2017	
	Official	Optimal Linear Measure	Official	Optimal Linear Measure	Official	Optimal Linear Measure
China	10.4	8.5	9.0	5.6	6.9	5.4
India	6.6	5.9	7.4	6.6	7.3	6.4
Brazil	3.3	3.5	3.2	3.1	-1.6	-0.8
South Africa	3.4	3.5	1.9	2.1	1.0	2.0

Notes. 1992-2013 results are based on DMSP/OLS data and 2013-2017 based on VIIRS. Growth rates are geometric average.

Figure 8: Real GDP per capita: Economic Disruption and Restoration
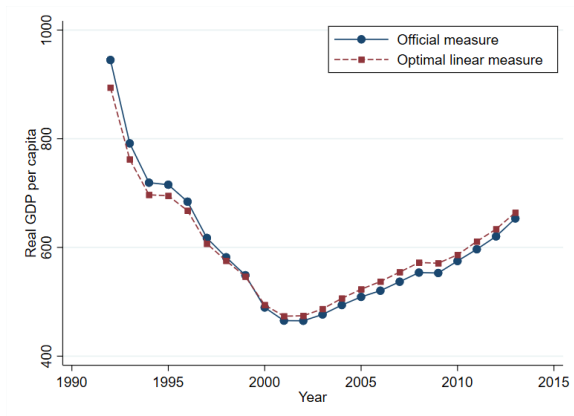
(a) Dem. Rep. of Congo
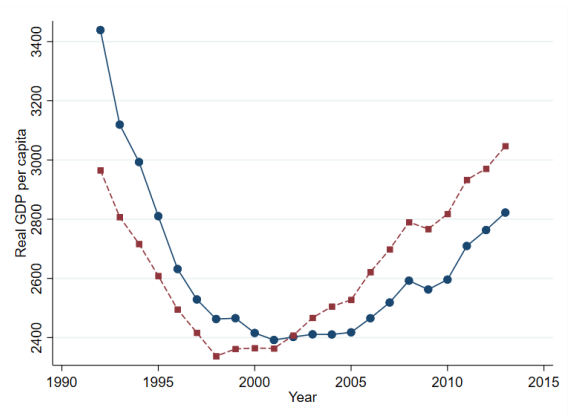
(b) Djibouti

(c) Kenya

(d) Sierra Leone

2001, panel (a) shows that the new measures of GDP per capita were worse than official figures suggested; to the contrary, when the economic situation improved afterwards, the new measures suggested higher living standards. Similarly, panel (b) shows that during the 1990s when armed conflicts routed the economy in Djibouti, the new measure suggested worse situation than official figures; when the economy recovered, the new measures suggested higher GDP per capita. Kenya's economy was afflicted by political instability before 2002 and Sierra Leone by its civil war in the 1990s. Graphs (c) and (d) again display a similar pattern of overestimation of real GDP per capita in the economic downturn and underestimation in the upturn. It is likely that periods of economic disruption made it difficult to track the economy accurately and the emergence of informal economy in subsequent restoration did not enter national accounts. We leave the precise mechanisms through which conflicts affect the economy for future research.

Appendix C.4 presents the official measures of real GDP per capita and our optimal linear measures for a number of other countries.

5.4.2 More on China's GDP

The quality of China's official statistics has been subject to frequent debate and skepticism. On the one hand, there is evidence that China's actual growth has been lower than official data suggest. For instance, the seminal article by Rawski [2001] argues that the Chinese economy might have grown at 2 percentage points less than officially claimed during 1997-2001. More recently, Chen et al. [2019], through examination of China's national accounts, find that GDP growth from 2010-2016 is 1.8 percentage points lower relative to official numbers.

On the other hand, many contends the opposite. Holz [2014] argues that the supposed evidence for China's GDP data falsification is not compelling. Fernald et al. [2013] focus on China's economic growth in 2012 and find no evidence that it was slower than official data indicate. Using data on trading-partner exports to China between 2000-2014, Fernald et al. [2015] find that the information content of Chinese GDP improves markedly after 2008. Clark et al. [2017], using forecast based on DMSP/OLS nighttime lights data, find that China's growth rates around 2015 were actually higher than officially reported.

To get a sense of how our results on China reconcile with the mixed findings in the literature, we conduct two exercises. First, Figure 9 reverses the construction of the optimal linear measure. The left graph shows that based on simple linear regression (9), nighttime-light predicted GDP indicates much lower growth rates than official

Figure 9: Optimal Linear Measure and Weight for China


| (a) Optimal Linear Measure | (b) Weight |
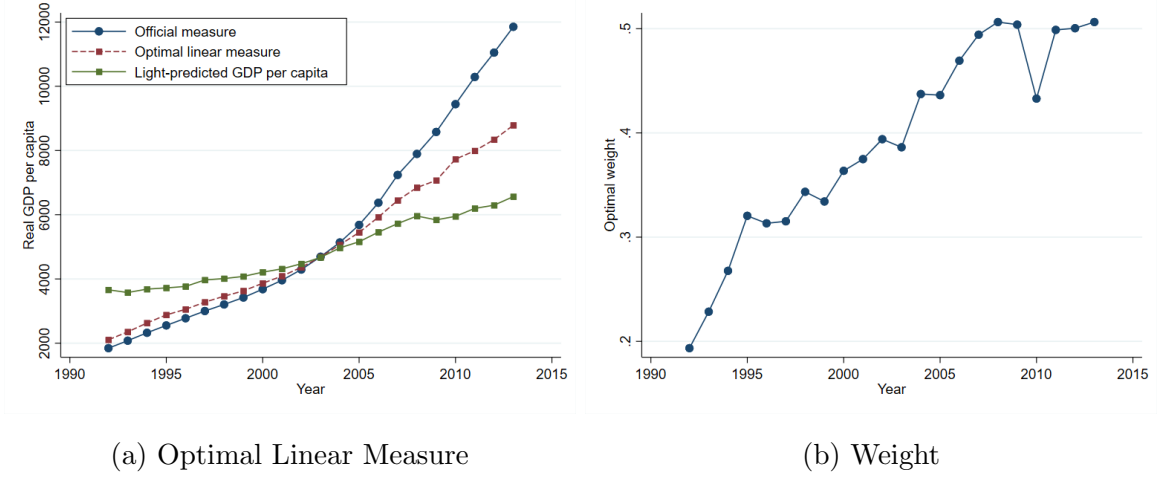
data. The right graph shows that our model puts increasing weight on prediction by nighttime lights. In other words, the lower growth rates implied in our optimal linear measure come from information in nighttime lights. The divergence between official data and our optimal linear measure after 2008 results from the increasing weight our model puts on nighttime lights.

Second, Figure 10 adds three additional estimators. The first estimator, $E[y^*|y, z, s, l]$, which is the semiparametric conditional mean, also points to an economic slowdown after 2005 as indicated by the optimal linear measure. Though the semiparametric conditional mean makes full use of the information in the conditional distributions, it can be volatile given limited data. The second estimator, $E[y^*|y, s]$, is the expected true value of real GDP per capita conditional only on official data. Note that it is actually above official data after 2005. This is consistent with the findings in the literature from China's own time series data that its GDP is similar to or even higher than official figures. The third estimator, $E[y^*|z, l]$, is the expected true value of real GDP per capita conditional only on nighttime lights data. It shows that based on the cross-country relationship between nighttime lights and GDP, China's nighttime lights suggest that its real GDP per capita was much lower than official data.[15] This is also consistent with the findings in the literature drawn from cross-country comparisons that China's GDP might have been lower than official data.

---

[15]The sudden jump in 2010 was because of a change of satellites (from F16 to F18) that resulted in an increase in the recorded nighttime lights for most countries. See `https://ngdc.noaa.gov/eog/dmsp/downloadV4composites.html`. While $E[y^*|z, l]$ increases accordingly, the optimal linear measure and the semiparametric conditional mean discount such increase by combining information from y.

Figure 10: Comparison between New Measures: China
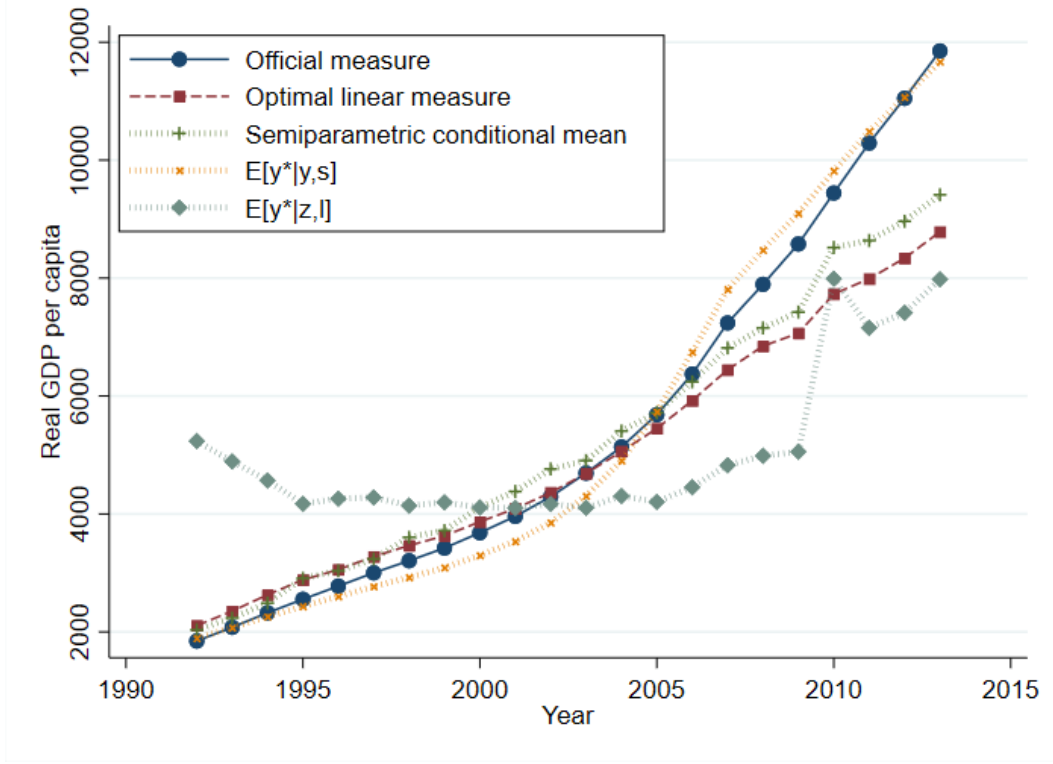
There could be many reasons for why nighttime lights suggest lower growth rates in China. Issues in national accounts, over-investment, under-utilization of capital, among others, can all be contributing factors. While it is beyond the scope of this paper to explore the exact channels, we highlight that nighttime lights provide a unique perspective on China's growth rate puzzle. It is worth pointing out that China is not an outlier in our data sets. In fact, Appendix D.1 shows that it is right in the middle.

5.5 Including Covariates

So far we have only explored the relationship between nighttime lights and GDP in a measurement error model framework. Next we extend our analysis to include additional covariates that might influence night light intensity and true real GDP per capita.

First, we include variables that capture certain characteristics of the economy that affect the use of lights at night, such as its electric power generation capacity or the size of the informal economy. Following the same notations as in equations 2 and 1 but omitting subscripts, we assume

$$Z = \theta_0 + \theta_1 Y^* + \theta_2 (Y^*)^2 + \kappa Q + \epsilon^Z(l) \tag{13}$$

31

where Q is the set of variables affecting nighttime lights beyond true real GDP per capita. Second, we add variables that are plausibly correlated with true real GDP per capita, including statistical capacity and country locations, as well as a set of measures of governance related development indicators – rule of law, control of corruption, and political stability,

$$Y = Y^* + \epsilon^Y(s), \tag{14}$$

$$Y^* = \delta_0 + \delta_1 S + \delta_2 L + \delta_w W + u, \tag{15}$$

where W is the set of development indicators.

It can be shown that θ's are identified in this setup. Because Y^* is unknown, coefficients in equations (13) and (15) have to be estimated through sieve MLE. Nevertheless, we present some constructive results from simple regressions. Table 12 explores the nonlinear relationship between night light intensity and real GDP per capita when additional covariates are added.[16] Columns (3) and (4) show that given the same level of income, countries with more installed power capacity are brighter at night. Countries with a larger agriculture sector, or a larger informal sector for which the agricultural share of the economy is a proxy, are less bright. However, the nonlinear relationship between night light intensity and real GDP per capita holds when such structural differences are accounted for.

Table 13 presents the results from sieve MLE. Notably, the quadratic term in real GDP per capita (θ_2) remains statistically significant.

We repeat the same exercises of constructing new measures of real GDP per capita but adding covariates in the predictive equation:

$$
\begin{aligned}
\hat{Y} &= \hat{\beta}_1 Z + \hat{\beta}_2 Z^2 + X\hat{\beta} \\
\hat{Y^*} &= \lambda \hat{Y} + (1 - \lambda) Y
\end{aligned}
$$

where X is the set of covariates including statistical capacity, country location, all variables in Q and W, and a constant. We find very similar results in terms of the optimal weights on light-predicted GDP. Our results regarding the difference between new measures and official measures hold for countries such as China and India, as well as conflict-disrupted economies such as Kenya and Sierra Leone. Intuitively, adding covariates change little the predictions by nighttime lights because nighttime lights, along with country and year fixed effects, already account for 98% variations in real

---

[16]On the data, we use total net installed capacity of electric power plants from the United Nations. The rest, including agricultural share and development indicators are from the World Bank.

Table 12: Nighttime Lights (DMSP/OLS) and Real GDP
1992-2013 with Covariates

	(1)	(2)	(3)	(4)
	Night Light Intensity			
(log) real GDP per capita	4.163***	1.956***	3.394***	1.090***
	(0.143)	(0.137)	(0.152)	(0.152)
(log) real GDP per capita squared	-0.171***	-0.0928***	-0.138***	-0.0305***
	(0.00800)	(0.00780)	(0.00815)	(0.00872)
installed capacity			0.0959***	0.162***
			(0.00567)	(0.0143)
agricultural share			-0.00969***	-0.00396***
			(0.00180)	(0.000954)
country FE	-	Yes	-	Yes
year FE	-	Yes	-	Yes
Obs	3870	3870	3616	3615
Adjusted R^2	0.751	0.983	0.791	0.986

Standard errors are in parentheses.

* $p < 0.10$, ** $p < 0.05$, *** $p < 0.01$

Table 13: Estimated Light Production Function with Covariates (DMSP/OLS)

Parameter	θ_1	θ_2	installed capacity	agricultural share	statistical capacity	latitude	rule of law	control of corruption	political stability
Point Estimate	0.986	-0.181	0.001	-0.017	0.135	0.606	0.653	0.060	0.179
Standard Error	(0.027)	(0.011)	(0.008)	(0.002)	(0.032)	(0.040)	(0.027)	(0.024)	(0.035)

Notes: Standard errors are based on 200 sample bootstraps.

GDP per capita.[17] Since the weights on light-predicted GDP only change slightly, so does the optimal linear combination.

6   Conclusion

In this paper, we first provide a statistical framework to describe the relationship among nighttime lights, official real GDP per capita, and true real GDP per capita. We make use of the variation of observed nighttime lights and official GDP across different statistical capacity and geographic location, and provide sufficient conditions under which the joint distribution of observables and the latent true GDP is uniquely determined by the distribution of observables. We obtain elasticity estimates of nighttime lights to real GDP between 0 and 2.3 depending on countries' income levels. We find that official real GDP per capita measures are less precise for low and middle income countries, and nighttime lights can play a bigger role in improving such measures. Based on estimated distributions, we construct new measures of real GDP per capita and real GDP growth. Comparing our new measures with official measures, we find that there are two types of discrepancy: systemic recording difference and poor measurement due to economic disruption. In particular, we find that China's real GDP growth has been consistently below official figures. We expect our statistical framework and methodology will have a broad impact on measuring GDP using additional information.

References

Alberto Alesina, Stelios Michalopoulos, and Elias Papaioannou. Ethnic inequality. *Journal of Political Economy*, 124(2):428–488, 2016.

S Borağan Aruoba, Francis X Diebold, Jeremy Nalewaik, Frank Schorfheide, and Dongho Song. Improving gdp measurement: A measurement-error perspective. *Journal of Econometrics*, 191(2):384–397, 2016.

Raymond J Carroll, Xiaohong Chen, and Yingyao Hu. Identification and estimation of nonlinear models using two samples with nonclassical measurement errors. *Journal of Nonparametric Statistics*, 22(4):379–399, 2010.

Wei Chen, Xilu Chen, Chang-Tai Hsieh, and Zheng Song. A forensic examination of china's national accounts. *NBER Working Paper No. w25754*, 2019.

---

[17]R^2 for regression (8) is above 0.98.

Xi Chen and William D Nordhaus. Using luminosity data as a proxy for economic statistics. *Proceedings of the National Academy of Sciences*, 108(21):8589–8594, 2011.

Hunter Clark, Maxim Pinkovskiy, and Xavier Sala-i Martin. China's gdp growth may be understated. Working Paper 23323, National Bureau of Economic Research, April 2017. URL http://www.nber.org/papers/w23323.

Dave Donaldson and Adam Storeygard. The view from above: Applications of satellite data in economics. *Journal of Economic Perspectives*, 30(4):171–98, 2016.

Nelson Dunford and Jacob T Schwartz. *Linear Operators Part 3: Spectral Operators*, volume 7. NewYork: JohnWiley & Sons, 1971.

Christopher D Elvidge, Kimberly E Baugh, Eric A Kihn, Herbert W Kroehl, and Ethan R Davis. Mapping city lights with nighttime data from the dmsp operational linescan system. *Photogrammetric Engineering and Remote Sensing*, 63(6):727–734, 1997.

Christopher D Elvidge, Edward H Erwin, Kimberly E Baugh, Daniel Ziskin, Benjamin T Tuttle, Tilottama Ghosh, and Paul C Sutton. Overview of dmsp nightime lights and future possibilities. In *Urban remote sensing event, 2009 joint*, pages 1–5. IEEE, 2009.

Shuaizhang Feng and Yingyao Hu. Misclassification errors and the underestimation of the us unemployment rate. *American Economic Review*, 103(2):1054–70, 2013.

John Fernald, Israel Malkin, Mark Spiegel, et al. On the reliability of chinese output figures. *FRBSF Economic Letter*, 8:1–5, 2013.

John G Fernald, Eric Hsu, and Mark M Spiegel. Is china fudging its figures? evidence from trading partner data. *Federal Reserve Bank of San Francisco Working Paper*, 12, 2015.

Joachim Freyberger. On completeness and consistency in nonparametric instrumental variable models. *Econometrica*, 85(5):1629–1644, 2017.

Tilottama Ghosh, Rebecca L Powell, Christopher D Elvidge, Kimberly E Baugh, Paul C Sutton, and Sharolyn Anderson. Shedding light on the global distribution of economic activity. *Open Geography Journal*, 3:147–160, 2010.

J Vernon Henderson, Adam Storeygard, and David N Weil. Measuring economic growth from outer space. *American Economic Review*, 102(2):994–1028, 2012.

J Vernon Henderson, Tim Squires, Adam Storeygard, and David Weil. The global distribution of economic activity: Nature, history, and the role of trade. *The Quarterly Journal of Economics*, 133(1):357–406, 2018. doi: 10.1093/qje/qjx030. URL `http://dx.doi.org/10.1093/qje/qjx030`.

Carsten A Holz. The quality of china's gdp statistics. *China Economic Review*, 30: 309–338, 2014.

Feng-Chi Hsu, Kimberly Baugh, Tilottama Ghosh, Mikhail Zhizhin, and Christopher Elvidge. Dmsp-ols radiance calibrated nighttime lights time series with intercalibration. *Remote Sensing*, 7(2):1855–1876, 2015.

Yingyao Hu. The econometrics of unobservables: Applications of measurement error models in empirical industrial organization and labor economics. *Journal of Econometrics*, 200(2):154–168, 2017.

Yingyao Hu and Susanne M Schennach. Instrumental variable treatment of nonclassical measurement error models. *Econometrica*, 76(1):195–216, 2008.

Luis R Martinez. How much should we trust the dictator's gdp estimates? *University of Chicago Working paper*, 2018. URL `https://ssrn.com/abstract=3093296`.

Maxim Pinkovskiy and Xavier Sala-i Martin. Lights, camera . . . income! illuminating the national accounts-household surveys debate. *The Quarterly Journal of Economics*, 131(2):579–631, 2016.

Thomas G Rawski. What is happening to china's gdp statistics? *China Economic Review*, 12(4):347–354, 2001.

Susanne M Schennach and Yingyao Hu. Nonparametric identification and semiparametric estimation of classical measurement error models without side information. *Journal of the American Statistical Association*, 108(501):177–186, 2013.

Xiaotong Shen and Wing Hung Wong. Convergence rate of sieve estimates. *The Annals of Statistics*, pages 580–615, 1994.

Kaifang Shi, Bailang Yu, Yixiu Huang, Yingjie Hu, Bing Yin, Zuoqi Chen, Liujia Chen, and Jianping Wu. Evaluating the ability of npp-viirs nighttime light data to

etimate the gross domestic product and the electric power consumption of china at multiple scales: A comparison with dmsp-ols data. *Remote Sensing*, 6(2):1705–1724, 2014.

Adam Storeygard. Farther on down the road: Transport costs, trade and urban growth in sub-saharan africa. *The Review of Economic Studies*, 83(3):1263–1295, 2016.

Appendices

A   More Details on Nighttime Lights Data

A.1   DMSP/OLS and VIIRS

The U.S. Air Force Defense Meteorological Satellite Program (DMSP) Operational Linescan System (OLS) has been collecting global low light imaging data since the 1970s. The National Oceanic and Atmospheric Administration (NOAA) processes the data and hosts a digital archive from 1992 to 2013.[18] DMSP satellites overpass at local

---

[18]The lights data can be downloaded here: `http://ngdc.noaa.gov/eog/dmsp/` `downloadV4composites.html`.

time in the 7pm to 9pm range,[19] and nighttime lights are a class of derived products of the low light imaging data in spectral bands where electric lights emissions are observed. NOAA provides cloud-free composites of nighttime lights based on a set of quality criteria that remove observations affected by sunlight, moonlight, glare, aurora, and the edges of the DMSP/OLS swaths.[20] For some years, there were two satellites collecting data and two composites were produced. In those cases, we use the average of the two composites. Each pixel of the DMSP/OLS nighttime lights images is a 30 arc-second grid (a bit less than 1 square kilometer). It is associated with a digital number from 0 to 63 that is increasing with brightness.

Since April 2012, nighttime lights data are produced monthly by the Visible Infrared Imaging Radiometer Suite (VIIRS) onboard a different satellite (Suomi-NPP).[21] VIIRS nighttime lights have a number of advantages compared to DMSP/OLS, including greater radiometric accuracy, finer geographical resolution, etc. The satellite's overpass time is after midnight. For our analysis, we take the annual averages of monthly data and treat them as annual data. In addition to VIIRS monthly composites, NOOA provides VIIRS annual composites for 2015 and 2016, but because of its limited sample size, we use it only for cross-checks.

A.2 Distributions

DMSP/OLS nighttime lights are top-coded as a result of sensor saturation, often raising concerns about their validity as a proxy for economic activity. We examine this issue using data in 2013, which is the brightest year in the DMSP/OLS sample – given that the world economy is growing and the world generally becomes brighter over time.

Figure 11 presents the distributions of nighttime lights in 2013 for a selected few countries representative of distinct country types. For each country, we count the number of pixels at each discrete value $(1, 2, \cdots, 63)$ and calculate its share of all pixels with positive values. For mainland China, the maximum value (63) accounts for only 1.07% of all lit pixels. For the United States, it is 2.37%. Singapore has 81.2% of lit pixels reach saturation while Sierra Leone has none. This example highlights that top coding in DMSP/OLS nighttime lights makes it not suitable for studying

---

[19]See Elvidge et al. [2009] for an overview.

[20]A detailed description of the selection criteria can be found here: `https://www.ngdc.noaa.gov/eog/gcv4_readme.txt`.

[21]VIIRS nighttime lights data can be downloaded here: `https://www.ngdc.noaa.gov/eog/viirs/download_dnb_composites_iframe.html`.

high-income cities or city states, which tend to have quality statistics anyway, but may be much less of a problem if the focus is on low and middle income countries or even advanced countries with large rural areas.

Figure 11: 2013 DMSP/OLS Nighttime Lights Distributions

(a) China (mainland)

(b) United States

(c) Sierra Leone

(d) Singapore
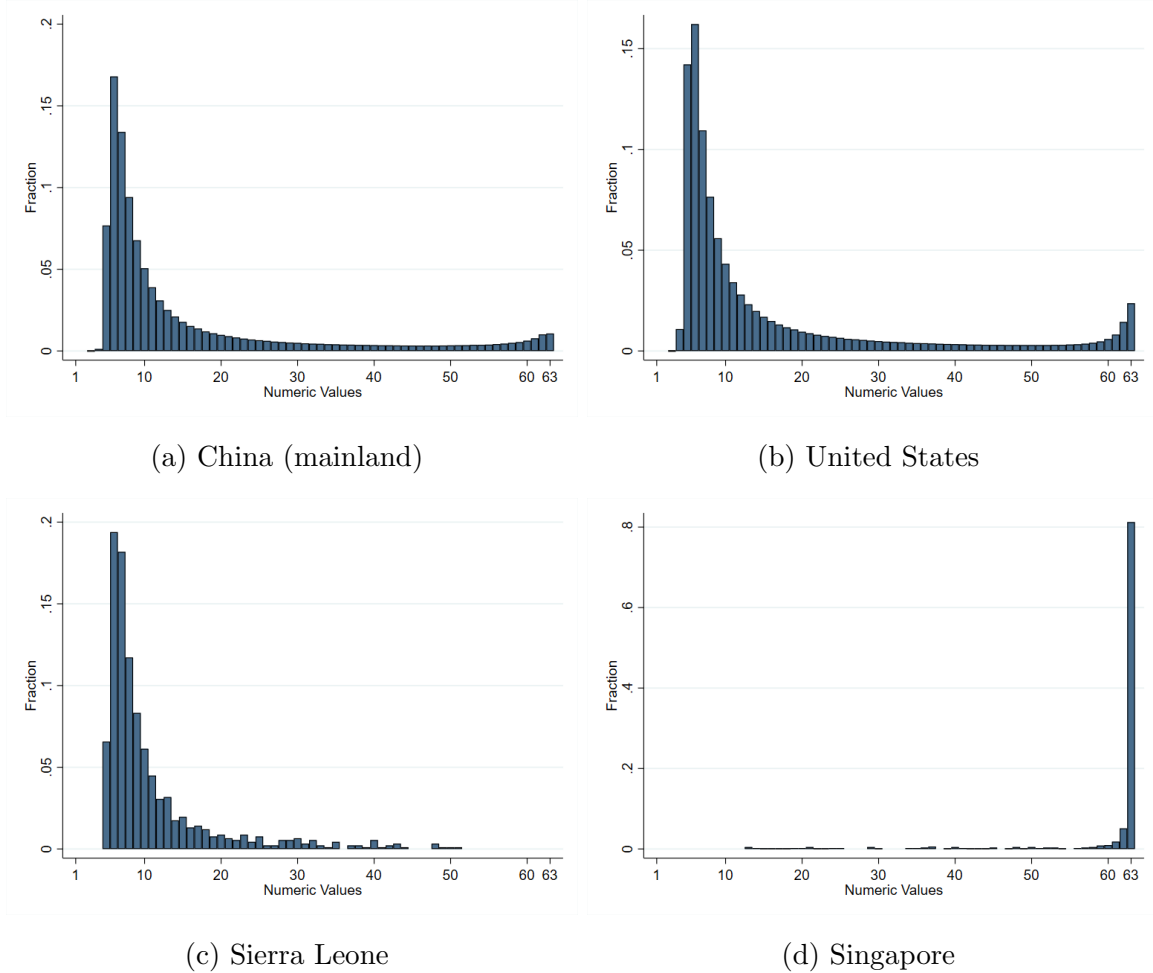
By comparison, Figure 12 presents the distributions of nighttime lights in 2016 VIIRS annual composites. As can be seen from the shapes of the distributions, they are not top-coded. For ease of reading, we do not show values above 40 for mainland China and the United States, which are almost zero fraction of all lit pixels. Instead, in Table 14, we show several percentiles of the distributions as well as the maximum numeric value of all pixels for each country. Note that the brightest pixel in the United States has a numeric value of 4006.38, which is orders-of-magnitude lower than the saturation value of VIIRS sensors (in the order of 10^7). In other words, VIIRS data can essentially be viewed as not top-coded.

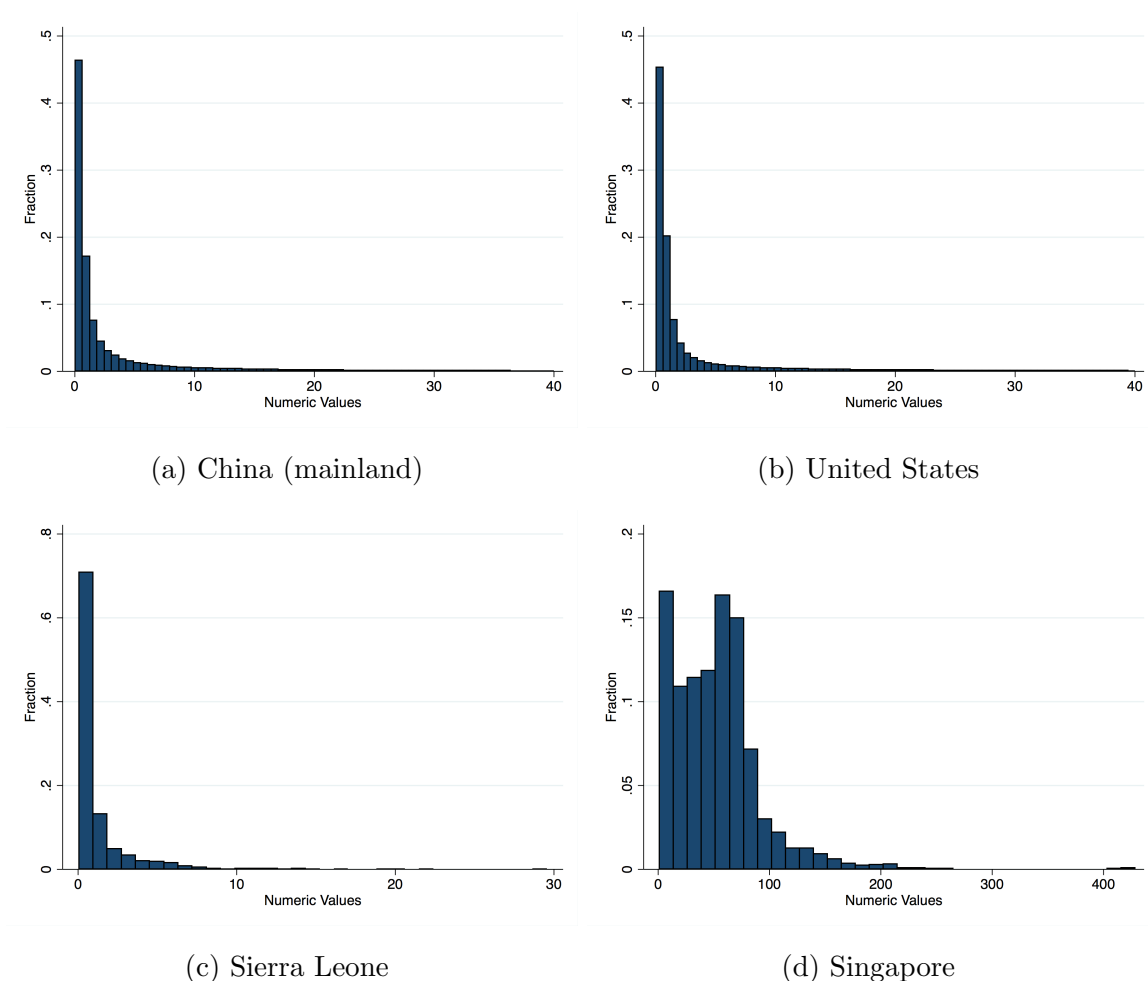Figure 12: 2016 VIIRS Annual Nighttime Lights Distributions

(a) China (mainland)

(b) United States

(c) Sierra Leone

(d) Singapore

Table 14: 2016 VIIRS Annual Nighttime Lights Distributions

Percentile	China (mainland)	United States	Singapore	Sierra Leone
1st	0.11	0.16	3.57	0.08
25th	0.35	0.40	24.11	0.24
50th	0.75	0.73	50.94	0.49
75th	2.48	2.23	70.08	1.10
99th	37.52	54.66	184.07	8.26
mean	3.41	4.23	52.30	1.16
max	1503.64	4006.38	428.23	29.56

Notes: Unit is nano Watts/cm^2/sr. Note that VIIRS satellite sensors can record up to 10^7 nano Watts/cm^2/sr, well above the max value for the selected countries in the table.

A.3 Gas Flaring in the Data

While nighttime lights primarily reflect economic activities for a majority of countries, it is recognized in the literature (for example, Henderson et al. [2012]) that the flaring of natural gas might make nighttime lights incommensurate with the level of economic development. To examine the extent to which gas flares affect our results, we use gas flare shapefiles (polygons) provided by NOOA[22] and calculate the fraction of nighttime lights within gas flare shapefiles in a country.

As an example, Figure 13 shows a map of Nigeria where the white area is the shapefile that contains gas flares and the green area is the rest of the country. We obtain the fraction of nighttime lights in gas flare shapefiles (denoted by τ) by aggregating the nighttime lights within the white area first and then divide the sum by the total sum of lights in Nigeria.
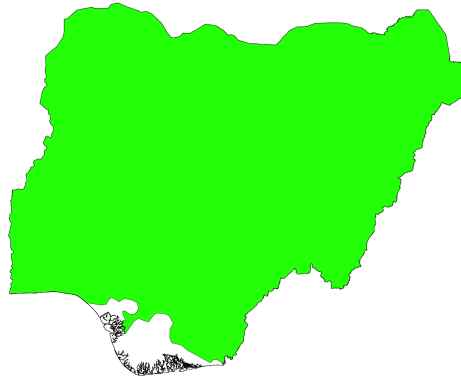
Figure 13: Gas Flares in Nigeria

Table 15 ranks countries by the fraction of nighttime lights in gas flare shapefiles in descending order. Among the highest are Equatorial Guinea, Gabon, and Nigeria. Most of the countries with high ranks are African and Middle East oil producers. While China and the United States produce oil, the vast majority of nighttime lights were produced in areas outside of the gas flare shapefiles. In particular, nighttime lights within gas flare shapefiles account for about 1 percent of total nighttime lights in China between 1992-2013 and even less for the United States. When dropping countries with $\tau \geq 0.02$ (34 countries) and reestimating our model, we find no statistically significant difference in estimated coefficients of the nighttime light production function compared to the full sample.

---

[22]https://ngdc.noaa.gov/eog/interest/gas_flares_countries_shapefiles.html

Table 15: Fraction of Nighttime Lights in Gas Flare Shapefiles

ISO code	τ	ISO code	τ	ISO code	τ	ISO code	τ
GNQ	0.75	RUS	0.17	VEN	0.08	AUS	0.01
GAB	0.69	AGO	0.16	ARE	0.06	CHN	0.01
NGA	0.57	SYR	0.15	SAU	0.05	CMR	0.01
LBY	0.36	ECU	0.15	EGY	0.04	MYS	0.00
IRQ	0.32	TKM	0.15	ARG	0.04	USA	0.00
KWT	0.31	TCD	0.14	SDN	0.03	ZAF	0.00
OMN	0.31	BOL	0.13	COL	0.03	PHL	0.00
DZA	0.30	PNG	0.13	CHL	0.03	BRA	0.00
COG	0.26	COD	0.11	PER	0.02	NOR	0.00
QAT	0.26	IRN	0.10	TUN	0.02	TTO	0.00
KAZ	0.24	UZB	0.09	CAN	0.01	$\cdots$	$\cdots$
YEM	0.20	IDN	0.09	AZE	0.01	$\cdots$	$\cdots$

Notes: τ is the ratio of the sum of nighttime lights in gas flare shapefiles to that in the whole country in DMSP/OLS data, averaged between 1992-2013.

B Mathematical Proofs

B.1 Technical Assumptions

In Section 4.2, we provide Theorem 1 that establishes nonparametric identification. In addition to Assumptions 1 and 2, we need four additional technical assumptions for Theorem 1 to hold, which we elaborate in this section.

We assume the existence of a random sample from distribution $f(z_{i,t}, y_{i,t}, s_i, l_i)$ for country i in year t. We provide sufficient conditions for the identification of latent distributions: $f(z_{i,t}|y^*_{i,t}, l_i)$, $f(y_{i,t}|y^*_{i,t}, s_i)$, and $f(y^*_{i,t}, s_i, l_i)$ from the observed distribution $f(z_{i,t}, y_{i,t}, s_i, l_i)$. In principle, both s and l can also be time-varying. In this subsection, we omit the subscript (i, t) for the simplicity of notations.

Suppose the supports of z, y, y^*, s, and l are $\mathcal{Z} \subseteq \mathbb{R}$, $\mathcal{Y} \subseteq \mathbb{R}$, $\mathcal{Y}^* \subseteq \mathbb{R}$, $\mathcal{S} = \{s_1, s_2, ..., s_J\}$ with $J \geq 2$, and $\mathcal{L} = \{l_1, l_2, ..., l_K\}$ with $K \geq 2$, respectively. We assume

Assumption 3 $f(z, y, y^*, s, l)$ is positive, bounded on its support $\mathcal{Z} \times \mathcal{Y} \times \mathcal{Y}^* \times \mathcal{S} \times \mathcal{L}$, and is continuous in $(z, y, y^*) \in \mathcal{Z} \times \mathcal{Y} \times \mathcal{Y}^*$.

Assumption 4 (i) for each given s, $\int f(y|y^*, s)h(y^*)dy^* = 0$ for all $y \in \mathcal{Y}$ for all bounded function h implies that $h \equiv 0$ over $\mathcal{Y}^*$; (ii) for each given (s, l), $\int f(z, y|s, l))h(y)dy = 0$, i.e., $E[h(y)|z, s, l] = 0$, for all $z \in \mathcal{Z}$ for all bounded function h implies that $h \equiv 0$ over $\mathcal{Y}$;

Assumption 4 (i) is the *bounded completeness* of the conditional density $f(y^*|y)$; see, e.g., Mattner (1993). Assumption 4 (ii) is imposed on observables directly and is directly testable under some restrictions (Freyberger [2017]). Nevertheless, comparing with conditions for parametric identification, Assumption 4 is a high level condition mainly because we are achieving a nonparametric identification result.

Define

$$\kappa^{jk}(y^*) \equiv \frac{f(y^*|s_a, l_j) f(y^*|s_b, l_k)}{f(y^*|s_b, l_j) f(y^*|s_a, l_k)} \quad \text{for } y^* \in \mathcal{Y}^*. \tag{16}$$

Assumption 5 *For any* $y_1^* \neq y_2^*$, *there exist* $j, k \in \{1, 2, ..., K\}$, *such that* $\kappa^{jk}(y_1^*) \neq \kappa^{jk}(y_2^*)$ *and* $\sup_{y^* \in \mathcal{Y}^*} \kappa^{jk}(y^*) < \infty$.

This assumption requires that the distribution of real GDP varies with countries' statistical capacity and geographic location, which is quite reasonable. In the data, we observe that higher income countries have more effective statistical institutions. In the meantime, it is well known that the GDP is highly correlated with countries' geographic location. Appendix D.2 provides more details on the data that underpin this assumption.

Since y^* is not observed, we need a normalization assumption as follows:

Assumption 6 *One of the followings holds for all* $y^* \in \mathcal{Y}^*$: *for some* s_j, *(i) (mean)* $E[y|y^*, s_j] = y^*$; *or (ii) (mode)* $\arg\max_y f(y|y^*, s_j) = y^*$; *or (iii) (median)* $\inf\{v : \int_{-\infty}^{v} f(y|y^*) \, dy \geq 0.5\} = y^*$.

Assumption 6 says that the reported GDP from some country with statistical capacity s_j is targeted for the true y^*. Specifically, either the mean, mode or median of the distribution of y given y^* and s_j is equal to y^*. This condition is <u>not</u> required for other countries with different statistical capacity.

Assumptions 1 and 2 are satisfied when the two error terms $\epsilon_{i,t}^y$ and $\epsilon_{i,t}^z$ are independent of each other and the latent true GDP. Assumption 3 holds when the distributions of the error terms and the latent true GDP are bounded and continuous and the function m is bounded and continuous. Assumption 4 is a high-level condition. Part (i) requires that the characteristic function of the error term $\epsilon_{i,t}^y$ does not varnish on the real line. Assumption 5 requires that the distribution of latent true GDP varies with statistical capacity and location. Assumption 6 requires that for some category fo the statistical capacity the error term $\epsilon_{i,t}^y$ has a zero mean, a zero mode, or a zero median.

Ideally, we should observe the statistical capacity $s_{i,t}$ for all the countries. The world bank, however, only provides this measure for middle and low income countries. Therefore, we assign an additional category for the discretized statistical capacity to represent the high income group. Since this assigned category coincides with the high income group, the support of the true GDP conditional on this category is different from the support of true GDP conditional on different statistical capacity and location in the middle or low income group. That means the assigned category can't serve as j and k in Assumption 5.

In addition, identification of the error distribution corresponding to this assigned category has to rely on the baseline specification (equations (1) and (2)). We use

Theorem 1 in Schennach and Hu [2013] to show that the distributions of y^*, ϵ^y, and ϵ^z, and function $m(.)$ are identified under assumptions as follows: i) the errors ϵ^y and ϵ^z are mutually independent with a zero mean and also jointly independent of y^*; ii) the characteristic functions of y and z do not vanish on the real line; and iii) function $m(\cdot)$ is monotone and continuously differentiable, and does not belong to a particular parametric family, which includes linear functions. Given that these assumptions are relatively mild comparing with those in the existing literature, we adopt this simple specification instead of imputing the statistical capacity for the high income counties.

B.2 Identification

We define the integral operator $L_{y|y^*,s_a} : \mathcal{L}^2(\mathcal{Y}^*) \to \mathcal{L}^2(\mathcal{Y})$ as:

$$\{L_{y|y^*,s_a}h\}(y) = \int_{\mathcal{Y}^*} f_{y|y^*,s}(y|y^*,s_a)h(y^*)\,dy^* \quad \text{for any } h \in \mathcal{L}^2(\mathcal{Y}^*),\, y \in \mathcal{Y}.$$

where $\mathcal{L}^2(\mathcal{Y})$ denotes the space of functions with $\int_{\mathcal{Y}}|h(y)|^2 dy < \infty$. Similarly, we define

$$L_{y,z|s_a,l_j} : \mathcal{L}^2(\mathcal{Z}) \to \mathcal{L}^2(\mathcal{Y}), \quad (L_{y,z|s_a,l_j}h)(y) = \int f_{y,z|s,l}(y,z|s_a,l_j)h(z)\,dz,$$

$$L_{z|y^*,l_j} : \mathcal{L}^2(\mathcal{Z}) \to \mathcal{L}^2(\mathcal{Y}^*), \quad (L_{z|y^*,l_j}h)(y^*) = \int f_{z|y^*,l}(z|y^*,l_j)h(z)\,dz,$$

$$D_{y^*|s_a,l_j} : \mathcal{L}^2(\mathcal{Y}^*) \to \mathcal{L}^2(\mathcal{Y}^*), \quad (D_{y^*|s_a,l_j}h)(y^*) = f_{y^*|s,l}(y^*,s_a,l_j)h(y^*).$$

Notice that the operator $D_{y^*|s_a,l_j}$ is diagonal or multiplication operator, and the operator $L_{y,z|s_a,l_j}$ is observed from the data.

Proof of Theorem 1: For each value (s,l), assumptions 1 and 2 imply that

$$f_{y,z|s,l}(y,z|s_a,l_j) = \int f_{y|y^*,s}(y|y^*,s_a)f_{z|y^*,l}(z|y^*,l_j)f_{y^*|s,l}(y^*,s_a,l_j)dy^*, \quad (17)$$

$$f_{y,z|s,l}(y,z|s_b,l_j) = \int f_{y|y^*,s}(y|y^*,s_b)f_{z|y^*,l}(z|y^*,l_j)f_{y^*|s,l}(y^*,s_b,l_j)dy^*. \quad (18)$$

By equation (17) and the definition of the operators, we have, for any function $h \in \mathcal{L}^2(\mathcal{Z})$,

$$
\begin{aligned}
(L_{y,z|s_a,l_j}h)(y) &= \int f_{y,z|s,l}(y,z|s_a,l_j)h(z)\,dz \\
&= \int \left(\int f_{y|y^*,s}(y|y^*,s_a)f_{z|y^*,l}(z|y^*,l_j)f_{y^*|s,l}(y^*,s_a,l_j)dy^* \right)h(z)\,dz \\
&= \int f_{y|y^*,s}(y|y^*,s_a)f_{y^*|s,l}(y^*,s_a,l_j)\left(\int f_{z|y^*,l}(z|y^*,l_j)h(z)\,dz \right)dy^* \\
&= \int f_{y|y^*,s}(y|y^*,s_a)f_{y^*|s,l}(y^*,s_a,l_j)(L_{z|y^*,l_j}h)(y^*)dy^* \\
&= \int f_{y|y^*,s}(y|y^*,s_a)(D_{y^*|s_a,l_j}L_{z|y^*,l_j}h)(y^*)dy^* \\
&= (L_{y|y^*,s_a}D_{y^*|s_a,l_j}L_{z|y^*,l_j}h)(y).
\end{aligned}
$$

This means we have the operator equivalence

$$L_{y,z|s_a,l_j} = L_{y|y^*,s_a} D_{y^*|s_a,l_j} L_{z|y^*,l_j}. \tag{19}$$

Similarly, we have,

$$L_{y,z|s_b,l_j} = L_{y|y^*,s_b} D_{y^*|s_b,l_j} L_{z|y^*,l_j}. \tag{20}$$

Note that the left-hand sides of equations (19) and (20) are observed.

Assumption 4 imply that all the operators involved in equations (19) and (20) are invertible. Hence

$$L_{y,z|s_a,l_j} L_{y,z|s_b,l_j}^{-1} = L_{y|y^*,s_a} D_{y^*|s_a,l_j} D_{y^*|s_b,l_j}^{-1} L_{y|y^*,s_b}^{-1}. \tag{21}$$

This equation holds for all s_j and s_k so that we may then eliminate $L_{y|y^*,s_b}$ to have

$$L_{y,y}^{jk} \equiv (L_{y,z|s_a,l_j} L_{y,z|s_b,l_j}^{-1})(L_{y,z|s_a,l_k} L_{y,z|s_b,l_k}^{-1})^{-1} = L_{y|y^*,s_a} D_{y^*}^{jk} L_{y|y^*,s_a}^{-1}, \tag{22}$$

where $D_{y^*}^{jk} : \mathcal{L}^2(\mathcal{Y}^*) \to \mathcal{L}^2(\mathcal{Y}^*)$ is still a diagonal operator

$$D_{y^*}^{jk} \equiv D_{y^*|s_a,l_j} D_{y^*|s_b,l_j}^{-1} (D_{y^*|s_a,l_k} D_{y^*|s_b,l_k}^{-1})^{-1}. \tag{23}$$

In fact, this diagonal operator can be defined as $(D_{y^*}^{jk}h)(y^*) \equiv \kappa^{jk}(y^*)h(y^*)$ with κ^{jk} defined in equation (16). Equation (22) implies a diagonalization of an observed operator $L_{y,y}^{jk}$, where an eigenvalue of $L_{y,y}^{jk}$ equals $\kappa^{jk}(y^*)$ for a value of y^* with corresponding eigenfunction $f_{y|y^*,s}(\cdot|y^*,s_a)$. Notice that each eigenfunction is a conditional density, and therefore, is automatically normalized.

Equation (22) implies that the operator $L_{y,y}^{jk}$ has the same spectrum as the diagonal operator $D_{y^*}^{jk}$. Since an operator is bounded by the largest element of its spectrum, Assumption 4 guarantees that the operator $L_{y,y}^{jk}$ is bounded with distinctive eigenvalues. Following theorem XV.4.3.5 in Dunford and Schwartz [1971], we have that the diagonal decomposition of $L_{y,y}^{jk}$ is unique up to the index of eigenvalues and eigenfunctions. Notice that Assumption 4 guarantees that, for any two different eigenfunctions $f_{y|y^*,s}(\cdot|y_1^*,s_a)$ and $f_{y|y^*,s}(\cdot|y_2^*,s_a)$, one can always find two subsets with l_j and l_k such that the two different eigenfunctions correspond to two different eigenvalues $\kappa^{jk}(y_1^*)$ and $\kappa^{jk}(y_2^*)$ and, therefore, are uniquely determined.

In order to fully identify each eigenfunction, we need to identify the exact value of y^* in each eigenfunction $f_{y|y^*,s}(\cdot|y^*,s_a)$. Here we use the ordering assumption in Hu and Schennach [2008], i.e. Assumption 6, to pin down the the exact value of y^* for each eigenfunction $f_{y|y^*,s}(\cdot|y^*,s_a)$. Such an identification procedure can be applied to each subpopulation with a different value of s. Thus, we have fully identified the conditional density $f_{y|y^*,s}$.

Given $f_{y|y^*,s}$, other densities containing y^* can also be identified due to the injectivitiy of operator $L_{y|y^*,s}$ as follows:

$$f_{z,y^*,s,l} = L_{y|y^*,s}^{-1} f_{z,y,s,l} \tag{24}$$

In summary, we have shown that the density $f(z,y,s,l)$ uniquely determines the joint density $f(z,y,y^*,s,l)$ satisfying $f(z,y,y^*,s,l) = f(y|y^*,s)f(z,y^*,s,l)$.

B.3 Sieve Maximum Likelihood Estimation

Given the general nonparametric identification, we provide a semiparametric estimator as suggested in Carroll et al. [2010]. We develop our estimator based on an i.i.d sample, which can be extended to for time series data. We assume that there is a random sample $\{z_i, y_i, s_i, l_i\}_{i=1}^n$.

We adopt a parametric specification of function $m(\cdot; \theta)$ and leave other elements nonparametrically specified in the simple specification in equations (1) and (2). Let the true value of the unknowns be $\alpha_0 \equiv (\theta_0^T, f_{01}, f_{02}, f_{03})^T \equiv (\theta_0^T, f_{y^*|s,l}, f_{\epsilon^y|s}, f_{\epsilon^z|l})^T$, where $f_{A|B}$ denotes the distribution of A conditional on B. We then introduce a sieve MLE estimator $\widehat{\alpha}$ for α_0, and establish the asymptotic normality of $\widehat{\theta}$. These results can also be extended to the case where the function m is misspecified.

Following Carroll et al. [2010], we consider the widely used Hölder space of functions. Let $\xi = (\xi_1, \xi_2, \xi_3)^T \in \mathbb{R}^3$, $a = (a_1, a_2, a_3)^T$, and $\nabla^a h(\xi) \equiv \frac{\partial^{a_1+a_2+a_3} h(\xi_1, \xi_2, \xi_3)}{\partial \xi_1^{a_1} \partial \xi_2^{a_2} \partial \xi_3^{a_3}}$ denote the $(a_1 + a_2 + a_3)^{\text{th}}$ derivative. Let $\|\cdot\|_E$ denote the Euclidean norm. Let $\mathcal{V} \subseteq \mathbb{R}^3$ and $\underline{\gamma}$ be the largest integer satisfying $\gamma > \underline{\gamma}$. The Hölder space $\Lambda^\gamma(\mathcal{V})$ of order $\gamma > 0$ is a space of functions $h : \mathcal{V} \mapsto \mathbb{R}$, such that the first $\underline{\gamma}$ derivatives are continuous and bounded, and the $\underline{\gamma}^{\text{th}}$ derivative is Hölder continuous with the exponent $\gamma - \underline{\gamma} \in (0, 1]$. We define a Hölder ball as $\Lambda_c^\gamma(\mathcal{V}) \equiv \{h \in \Lambda^\gamma(\mathcal{V}) : \|h\|_{\Lambda^\gamma} \le c < \infty\}$, in which

$$\|h\|_{\Lambda^\gamma} \equiv \max_{a_1+a_2+a_3 \le \underline{\gamma}} \sup_\xi |\nabla^a h(\xi)| + \max_{a_1+a_2+a_3 = \underline{\gamma}} \sup_{\xi \ne \xi'} \frac{|\nabla^a h(\xi) - \nabla^a h(\xi')|}{(\|\xi - \xi'\|_E)^{\gamma - \underline{\gamma}}} < \infty.$$

The space containing $f_{01} = f_{y^*|s,l}$ are assumed to be

$$\mathcal{F}_1 = \left\{ \begin{array}{l} f_1(\cdot|\cdot, \cdot) \in \Lambda_c^{\gamma_1} (\mathcal{Y}^* \times \mathcal{S} \times \mathcal{L}) : \text{Assumption 5 holds,} \\ f_3(\cdot|s, l) \text{ is a positive density function for all } s \in \mathcal{S}, l \in \mathcal{L} \end{array} \right\}.$$

Similarly, we assume f_{02} and f_{03} are in the following functional spaces

$$\mathcal{F}_2 = \left\{ \begin{array}{l} f_2(\cdot|\cdot) \in \Lambda_c^{\gamma_2} (\mathcal{E}^y \times \mathcal{S}) : \text{Assumption 6 holds,} \\ f_2(\cdot|s) \text{ is a positive density function for all } s \in \mathcal{S} \end{array} \right\},$$

and

$$\mathcal{F}_3 = \{f_3(\cdot|\cdot) \in \Lambda_c^{\gamma_3} (\mathcal{E}^z \times \mathcal{Z}) : f_3(\cdot|l) \text{ is a positive density function for all } l \in \mathcal{L}\},$$

where $\mathcal{E}^y$ and $\mathcal{E}^z$ are supports of the error terms in equations (1) and (2), respectively.

Let $\mathcal{A} = \Theta \times \mathcal{F}_1 \times \mathcal{F}_2 \times \mathcal{F}_3$ as the parameter space. The log-joint likelihood for $\alpha \equiv (\theta^T, f_1, f_2, f_3)^T \in \mathcal{A}$ is given by:

$$\sum_{i=1}^n \log f(z_i, y_i, s_i, l_i) = \sum_{i=1}^n \ell(D_i; \alpha),$$

in which $D_i = (z_i, y_i, s_i, l_i)$ and

$$\begin{aligned} \ell(D_i; \alpha) &\equiv \ell(z_i, y_i, s_i, l_i; \theta, f_1, f_2, f_3) \\ &= \log\{\int f_1(y^*|s_i, l_i) f_2(y_i - y^*|s_i) f_3(z_i - m(y^*; \theta)|l_i) dy^*\} + \log f(s_i, l_i). \end{aligned}$$

Let $E[\cdot]$ denote the expectation with respect to the underlying true data generating process for D_i. Then

$$\alpha_0 = \arg\sup_{\alpha \in \mathcal{A}} E\left[\ell(D_i; \alpha)\right].$$

We then use a sequence of finite-dimensional sieve spaces $\mathcal{A}_n = \Theta \times \mathcal{F}_1^n \times \mathcal{F}_2^n \times \mathcal{F}_3^n$ to approximate the functional space $\mathcal{A} = \Theta \times \mathcal{F}_1 \times \mathcal{F}_2 \times \mathcal{F}_3$. The semiparametric sieve MLE $\widehat{\alpha}_n = \left(\widehat{\theta}^T, \widehat{f}_1, \widehat{f}_2, \widehat{f}_3\right)^T \in \mathcal{A}_n$ for $\alpha_0 \in \mathcal{A}$ is defined as:

$$\widehat{\alpha}_n = \arg\max_{\alpha \in \mathcal{A}_n} \sum_{i=1}^{n} \ell(D_i; \alpha).$$

Let $p^{k_n}(\cdot)$ be a $k_n \times 1-$vector of known basis functions, such as power series, splines, Fourier series, Legendre polynomials, Hermite polynomials, etc. We use linear sieves to directly approximate unknown densities:

$$\mathcal{F}_1^n = \left\{ f_1(y^*|s,l) = \left[\sum_{i=1}^{K}\sum_{j=1}^{J} p^{k_{1,n}}(y^*)^T \beta_{1,i,j} I(l = l_i) I(s = s_j)\right]^2 \in \mathcal{F}_1 \right\}$$

$$\mathcal{F}_2^n = \left\{ f_2(e|s) = \left[\sum_{j=1}^{J} p^{k_{2,n}}(e)^T \beta_{2,j} I(s = s_j)\right]^2 \in \mathcal{F}_2 \right\}$$

$$\mathcal{F}_3^n = \left\{ f_3(e|l) = \left[\sum_{i=1}^{K} p^{k_{3,n}}(e)^T \beta_{3,i} I(l = l_i)\right]^2 \in \mathcal{F}_3 \right\}.$$

Below we present the asymptotic properties of the proposed estimator.

B.4   Consistency

Here we provide sufficient conditions for the consistency of the sieve estimator $\widehat{\alpha}_n = \left(\widehat{\theta}^T, \widehat{f}_1, \widehat{f}_2, \widehat{f}_3,\right)^T$.

Assumption 7 *(i) All the assumptions in theorem 1 hold; (ii) $f_{y^*|s,l}(\cdot|s,l) \in \mathcal{F}_1$ with $\gamma_1 > 1/2$ for all $s \in \mathcal{S}$ and $l \in \mathcal{L}$; (iii) $f_{\epsilon^y|s}(\cdot|\cdot) \in \mathcal{F}_2$ with $\gamma_2 > 1$; (iv) $f_{\epsilon^z|l}(\cdot|\cdot) \in \mathcal{F}_3$ with $\gamma_3 > 1$.*

Assumption 8 *(i) $\{z_i, y_i, s_i, l_i\}_{i=1}^{n}$ is i.i.d.; (ii) $m(y^*; \theta)$ is continuous in $\theta \in \Theta$, and Θ is a compact subset of $\mathbb{R}^{d_\theta}$; (iii) $\theta_0 \in \Theta$ is the unique solution of $E[z|y^*, l] = m(y^*; \theta)$ over $\theta \in \Theta$.*

We define a norm on $\mathcal{A}$ as: $\|\alpha\|_s = \|\theta\|_E + \|f_1\|_{\infty,\omega_1} + \|f_2\|_{\infty,\omega_2} + \|f_3\|_{\infty,\omega_3}$ in which $\|h\|_{\infty,\omega_j} \equiv \sup_\xi |h(\xi)\omega_j(\xi)|$ with $\omega_j(\xi) = \left(1 + \|\xi\|_E^2\right)^{-\varsigma_j/2}$, $\varsigma_j > 0$ for $j = 1, 2, 3$. We assume

Assumption 9 *(i)* $-\infty < E\left[\ell(D_i; \alpha_0)\right] < \infty$, $E\left[\ell(D_i; \alpha)\right]$ *is upper semicontinuous on* $\mathcal{A}$ *under the metric* $\|\cdot\|_s$; *(ii) there is a finite* $\tau > 0$ *and a random variable* $U(D_i)$ *with* $E\{U(D_i)\} < \infty$ *such that* $\sup_{\alpha \in \mathcal{A}_n : \|\alpha - \alpha_0\|_s \leq \delta} |\ell(D_i; \alpha) - \ell(D_i; \alpha_0)| \leq \delta^\tau U(D_i)$.

Assumption 10 *(i)* $p^{k_{j,n}}(\cdot)$ *is a* $k_{j,n} \times 1-$*vector of basis functions on* $\mathbb{R}$ *for* $j = 1, 2, 3$; *(ii)* $\min\{k_{1,n}, k_{2,n}, k_{3,n}\} \to \infty$ *and* $\max\{k_{1,n}, k_{2,n}, k_{3,n}\}/n \to 0$.

We then have

Lemma 1 Under Assumptions 7–10, we have $\|\widehat{\alpha}_n - \alpha_0\|_s = o_p(1)$.

This is a direct extension from Carroll et al. [2010] , which uses theorem 3.1 in Chen (2007).

B.5   Convergence Rates and Asymptotic Normality

The asymptotic properties of our estimator is a direct extension of that in Carroll et al. [2010]. We list the conditions below for readers' convenience.

B.5.1   Convergence Rates of Nonparametric Part

Given the consistency shown in Lemma 1, we focus on a shrinking $\|\cdot\|_s-$neighborhood around α_0. Let $\mathcal{A}_{0s} \equiv \{\alpha \in \mathcal{A} : \|\alpha - \alpha_0\|_s = o(1), \|\alpha\|_s \leq c_0 < c\}$ and $\mathcal{A}_{0sn} \equiv \{\alpha \in \mathcal{A}_n : \|\alpha - \alpha_0\|_s = o(1), \|\alpha\|_s \leq c_0 < c\}$. We assume that both $\mathcal{A}_{0s}$ and $\mathcal{A}_{0sn}$ are convex parameter spaces, and that $\ell(D_i; \alpha + \tau v)$ is twice continuously differentiable at $\tau = 0$ for almost all D_i and any direction $v \in \mathcal{A}_{0s}$.

Define the pathwise first and second derivatives of the sieve loglikelihood in the direction v as

$$\frac{d\ell(D_i; \alpha)}{d\alpha}[v] \equiv \frac{d\ell(D_i; \alpha + \tau v)}{d\tau}\Big|_{\tau=0}; \quad \frac{d^2\ell(D_i; \alpha)}{d\alpha d\alpha^T}[v, v] \equiv \frac{d^2\ell(D_i; \alpha + \tau v)}{d\tau^2}\Big|_{\tau=0}.$$

Mimicking Ai and Chen (2007), for any $\alpha_1, \alpha_2 \in \mathcal{A}_{0s}$, we define a pseudo metric $\|\cdot\|_2$ as

$$\|\alpha_1 - \alpha_2\|_2 \equiv \sqrt{-E\left(\frac{d^2\ell(D_i; \alpha_0)}{d\alpha d\alpha^T}[\alpha_1 - \alpha_2, \alpha_1 - \alpha_2]\right)}.$$

Our goal is to show that $\widehat{\alpha}_n$ converges to α_0 at a rate faster than $n^{-1/4}$ under the pseudo metric $\|\cdot\|_2$. We make the following assumptions:

Assumption 11 *(i)* $\varsigma_j > \gamma_j$ *for* $j = 1, 2, 3$; *(ii)* $\max\{k_{1,n}^{-\gamma_1/2}, k_{2,n}^{-\gamma_2/2}, k_{3,n}^{-\gamma_3}\} = o(n^{-1/4})$.

Assumption 12 *(i)* $\mathcal{A}_{0s}$ *is convex at* α_0 *and* $\theta_0 \in int(\Theta)$; *(ii)* $\ell(D_i; \alpha)$ *is twice continuously pathwise differentiable with respect to* $\alpha \in \mathcal{A}_{0s}$, *and* $m(y^*; \theta)$ *is twice continuously differentiable at* θ_0.

Assumption 13 $\sup_{\widetilde{\alpha} \in \mathcal{A}_{0s}} \sup_{\alpha \in \mathcal{A}_{0sn}} \left| \frac{d\ell(D_i; \widetilde{\alpha})}{d\alpha}\left[\frac{\alpha - \alpha_0}{\|\alpha - \alpha_0\|_s}\right] \right| \leq U(D_i)$ *for a random variable* $U(D_i)$ *with* $E\{[U(D_i)]^2\} < \infty$.

Assumption 14 *(i)* $\sup_{v \in \mathcal{A}_{0s}:\|v\|_s=1} -E\left(\frac{d^2\ell(D_i;\alpha_0)}{d\alpha d\alpha^T}[v,v]\right) \leq C < \infty$; *(ii) uniformly over* $\widetilde{\alpha} \in \mathcal{A}_{0s}$ *and* $\alpha \in \mathcal{A}_{0sn}$, *we have*

$$-E\left(\frac{d^2\ell(D_i;\widetilde{\alpha})}{d\alpha d\alpha^T}[\alpha - \alpha_0, \alpha - \alpha_0]\right) = \|\alpha - \alpha_0\|_2^2 \times \{1 + o(1)\}.$$

These assumptions are standard in the literature. As a direct application of Theorem 3.2 of Shen and Wong [1994] to the local parameter space $\mathcal{A}_{0s}$ and the local sieve space $\mathcal{A}_{0sn}$, we have

Theorem 2 Let $\gamma \equiv \min\{\gamma_1/2,\ \gamma_2/2,\ \gamma_3\} > 1/2$. Under assumptions 7–14, if $k_{1,n} = O\left(n^{\frac{1}{\gamma_1+1}}\right)$, $k_{2,n} = O\left(n^{\frac{1}{\gamma_2+1}}\right)$, and $k_{3,n} = O\left(n^{\frac{1}{2\gamma_3+1}}\right)$, then

$$\|\widehat{\alpha}_n - \alpha_0\|_2 = O_P\left(n^{\frac{-\gamma}{2\gamma+1}}\right) = o_P\left(n^{-1/4}\right).$$

B.5.2   Asymptotic Normality of Parametric Part

This section presents sufficient conditions for the asymptotic normality of the parametric part of the model. Define an inner product corresponding to the pseudo metric $\|\cdot\|_2$:

$$\langle v_1, v_2 \rangle_2 \equiv -E\left[\frac{d^2\ell(D_i;\alpha_0)}{d\alpha d\alpha^T}[v_1, v_2]\right],$$

where

$$\frac{d^2\ell(D_i;\alpha_0)}{d\alpha d\alpha^T}[v_1, v_2] \equiv \frac{d^2\ell(D_i;\alpha_0 + \tau_1 v_1 + \tau_2 v_2)}{d\tau_1 d\tau_2}\Big|_{\tau_1=\tau_2=0}.$$

Let $\overline{\mathbf{V}}$ denote the closure of the linear span of $\mathcal{A} - \{\alpha_0\}$ under the metric $\|\cdot\|_2$. Then $\left(\overline{\mathbf{V}}, \|\cdot\|_2\right)$ is a Hilbert space. We define $\overline{\mathbf{V}} = \mathbb{R}^{d_\theta} \times \overline{\mathcal{U}}$ with $\overline{\mathcal{U}} \equiv \overline{\mathcal{F}_1 \times \mathcal{F}_2 \times \mathcal{F}_3} - \{(f_{01}, f_{02}, f_{03})\}$ and let $h = (f_1, f_2, f_3)$ denote all the unknown densities. The pathwise first derivative can be written as

$$\begin{aligned}
\frac{d\ell(D_i;\alpha_0)}{d\alpha}[\alpha - \alpha_0] &= \frac{d\ell(D_i;\alpha_0)}{d\theta^T}(\theta - \theta_0) + \frac{d\ell(D_i;\alpha_0)}{dh}[h - h_0] \\
&= \left(\frac{d\ell(D_i;\alpha_0)}{d\theta^T} - \frac{d\ell(D;\alpha_0)}{dh}[\mu]\right)(\theta - \theta_0),
\end{aligned}$$

with $h - h_0 \equiv -\mu \times (\theta - \theta_0)$, and in which

$$\begin{aligned}
\frac{d\ell(D_i;\alpha_0)}{dh}[h - h_0] &= \frac{d\ell(D_i;\theta_0, h_0(1-\tau) + \tau h)}{d\tau}\Big|_{\tau=0} \\
&= \frac{d\ell(D_i;\alpha_0)}{df_1}[f_1 - f_{01}] + \frac{d\ell(D_i;\alpha_0)}{df_{1a}}[f_{1a} - f_{01a}] \\
&\quad + \frac{d\ell(D_i;\alpha_0)}{df_2}[f_2 - f_{02}] + \frac{d\ell(D_i;\alpha_0)}{df_{2a}}[f_{2a} - f_{02a}].
\end{aligned}$$

Note that

$$\begin{aligned}
&E\left(\frac{d^2\ell(D_i;\alpha_0)}{d\alpha d\alpha^T}[\alpha - \alpha_0, \alpha - \alpha_0]\right) \\
&= (\theta - \theta_0)^T E\left(\frac{d^2\ell(D_i;\alpha_0)}{d\theta d\theta^T} - 2\frac{d^2\ell(D_i;\alpha_0)}{d\theta dh^T}[\mu] + \frac{d^2\ell(D_i;\alpha_0)}{dh dh^T}[\mu, \mu]\right)(\theta - \theta_0),
\end{aligned}$$

with $h - h_0 \equiv -\mu \times (\theta - \theta_0)$, and in which

$$\frac{d^2\ell(D_i; \alpha_0)}{d\theta dh^T}[h - h_0] = \frac{d(\partial\ell(D_i; \theta_0, h_0(1 - \tau) + \tau h)/\partial\theta)}{d\tau}\Big|_{\tau=0},$$

$$\frac{d^2\ell(D_i; \alpha_0)}{dh dh^T}[h - h_0, h - h_0] = \frac{d^2\ell(D_i; \theta_0, h_0(1 - \tau) + \tau h)}{d\tau^2}\Big|_{\tau=0}.$$

For each component θ^k (of θ), $k = 1, ..., d_\theta$, suppose there exists a $\mu^{*k} \in \overline{\mathcal{U}}$ that solves:

$$\mu^{*k} : \inf_{\mu^k \in \overline{\mathcal{U}}} E\left\{ -\left(\frac{\partial^2\ell(D_i; \alpha_0)}{\partial\theta^k \partial\theta^k} - 2\frac{d^2\ell(D_i; \alpha_0)}{\partial\theta^k dh^T}[\mu^k] + \frac{d^2\ell(D_i; \alpha_0)}{dh dh^T}[\mu^k, \mu^k] \right) \right\}.$$

Denote $\mu^* = \left(\mu^{*1}, \mu^{*2}, ..., \mu^{*d_\theta}\right)$ with each $\mu^{*k} \in \overline{\mathcal{U}}$, and

$$\frac{d\ell(D_i; \alpha_0)}{dh}[\mu^*] = \left(\frac{d\ell(D_i; \alpha_0)}{dh}[\mu^{*1}], ..., \frac{d\ell(D_i; \alpha_0)}{dh}[\mu^{*d_\theta}] \right),$$

$$\frac{d^2\ell(D_i; \alpha_0)}{\partial\theta dh^T}[\mu^*] = \left(\frac{d^2\ell(D_i; \alpha_0)}{\partial\theta dh}[\mu^{*1}], ..., \frac{d^2\ell(D_i; \alpha_0)}{\partial\theta dh}[\mu^{*d_\theta}] \right),$$

$$\frac{d^2\ell(D_i; \alpha_0)}{dh dh^T}[\mu^*, \mu^*] = \begin{pmatrix} \frac{d^2\ell(D_i; \alpha_0)}{dh dh^T}[\mu^{*1}, \mu^{*1}] & \cdots & \frac{d^2\ell(D_i; \alpha_0)}{dh dh^T}[\mu^{*1}, \mu^{*d_\theta}] \\ \cdots & \cdots & \cdots \\ \frac{d^2\ell(D_i; \alpha_0)}{dh dh^T}[\mu^{*d_\theta}, \mu^{*1}] & \cdots & \frac{d^2\ell(D_i; \alpha_0)}{dh dh^T}[\mu^{*d_\theta}, \mu^{*d_\theta}] \end{pmatrix}.$$

We also define

$$V_* \equiv -E\left(\frac{\partial^2\ell(D_i; \alpha_0)}{\partial\theta \partial\theta^T} - 2\frac{d^2\ell(D_i; \alpha_0)}{\partial\theta dh^T}[\mu^*] + \frac{d^2\ell(D_i; \alpha_0)}{dh dh^T}[\mu^*, \mu^*] \right). \qquad (25)$$

We then consider a linear functional of α, which is $\lambda^T\theta$ for any $\lambda \in \mathbb{R}^{d_\theta}$ with $\lambda \neq 0$. Since

$$\sup_{\alpha - \alpha_0 \neq 0} \frac{|\lambda^T(\theta - \theta_0)|^2}{\|\alpha - \alpha_0\|_2^2}$$

$$= \sup_{\theta \neq \theta_0, \mu \neq 0} \frac{(\theta - \theta_0)^T \lambda\lambda^T(\theta - \theta_0)}{(\theta - \theta_0)^T E\left\{ -\left(\frac{d^2\ell(D_i; \alpha_0)}{d\theta d\theta^T} - 2\frac{d^2\ell(D_i; \alpha_0)}{d\theta dh^T}[\mu] + \frac{d^2\ell(D_i; \alpha_0)}{dh dh^T}[\mu, \mu] \right) \right\}(\theta - \theta_0)}$$

$$= \lambda^T(V_*)^{-1}\lambda,$$

the functional $\lambda^T(\theta - \theta_0)$ is *bounded* if and only if the matrix V_* is nonsingular.

Suppose that V_* is nonsingular. For any fixed $\lambda \neq 0$, denote $v^* \equiv (v_\theta^*, v_h^*)$ with $v_\theta^* \equiv (V_*)^{-1}\lambda$ and $v_h^* \equiv -\mu^* \times v_\theta^*$. Then the Riesz representation theorem implies: $\lambda^T(\theta - \theta_0) = \langle v^*, \alpha - \alpha_0 \rangle_2$ for all $\alpha \in \mathcal{A}$. We have:

$$\lambda^T(\widehat{\theta}_n - \theta_0) = \langle v^*, \widehat{\alpha}_n - \alpha_0 \rangle_2 \qquad (26)$$

$$= \frac{1}{n + n_a}\sum_{i=1}^n \frac{d\ell(D_i; \alpha_0)}{d\alpha}[v^*] + o_p\{n^{-1/2}\}.$$

51

Denote $\mathcal{N}_0 = \{\alpha \in \mathcal{A}_{0s} : \|\alpha - \alpha_0\|_2 = o(n^{-1/4})\}$ and $\mathcal{N}_{0n} = \{\alpha \in \mathcal{A}_{0sn} : \|\alpha - \alpha_0\|_2 = o(n^{-1/4})\}$. We provide additional sufficient for asymptotic normality of sieve MLE $\widehat{\theta}_n$ as follows:

Assumption 15 μ^* exists (i.e., $\mu^{*k} \in \overline{\mathcal{U}}$ for $k = 1, ..., d_\theta$), and V_* is positive-definite.

Assumption 16 There is a $v_n^* \in \mathcal{A}_n - \{\alpha_0\}$, such that $\|v_n^* - v^*\|_2 = o(1)$ and $\|v_n^* - v^*\|_2 \times \|\widehat{\alpha}_n - \alpha_0\|_2 = o_P(\frac{1}{\sqrt{n}})$.

Assumption 17 There is a random variable $U(D_i)$ with $E\{[U(D_i)]^2\} < \infty$ and a non-negative measurable function η with $\lim_{\delta \to 0} \eta(\delta) = 0$, such that, for all $\alpha \in \mathcal{N}_{0n}$,

$$\sup_{\overline{\alpha} \in \mathcal{N}_0} \left| \frac{d^2\ell(D_i; \overline{\alpha})}{d\alpha d\alpha^T}[\alpha - \alpha_0, v_n^*] \right| \leq U(D_i) \times \eta(\|\alpha - \alpha_0\|_s).$$

Assumption 18 Uniformly over $\overline{\alpha} \in \mathcal{N}_0$ and $\alpha \in \mathcal{N}_{0n}$,

$$E\left(\frac{d^2\ell(D_i; \overline{\alpha})}{d\alpha d\alpha^T}[\alpha - \alpha_0, v_n^*] - \frac{d^2\ell(D_i; \alpha_0)}{d\alpha d\alpha^T}[\alpha - \alpha_0, v_n^*] \right) = o\left(\frac{1}{\sqrt{n}}\right).$$

Assumption 19 $E\{\left(\frac{d\ell(D_i; \alpha_0)}{d\alpha}[v_n^* - v^*]\right)^2\}$ goes to zero as $\|v_n^* - v^*\|_2$ goes to zero.

Recall the definitions of Fisher inner product and the Fisher norm:

$$\langle v_1, v_2 \rangle \equiv E\left\{ \left(\frac{d\ell(D_i; \alpha_0)}{d\alpha}[v_1] \right) \left(\frac{d\ell(D_i; \alpha_0)}{d\alpha}[v_2] \right) \right\}, \quad \|v\| \equiv \sqrt{\langle v, v \rangle}.$$

Under correct specification, $m(y^*; \theta_0) = E(z|y^*, l)$, it can be shown that $\|v\| = \|v\|_2$ and $\langle v_1, v_2 \rangle = \langle v_1, v_2 \rangle_2$. Thus, the space $\overline{\mathbf{V}}$ is also the closure of the linear span of $\mathcal{A} - \{\alpha_0\}$ under the Fisher metric $\|\cdot\|$.

Suppose that θ has d_θ components, and write its kth component as θ^k. Write $\mu^* = \left(\mu^{*1}, \mu^{*2}, ..., \mu^{*d_\theta}\right)$, where we compute $\mu^{*k} \equiv \left(\mu_1^{*k}, \mu_2^{*k}, \mu_3^{*k}\right)^T \in \overline{\mathcal{U}}$ as the solution to

$$\inf_{\mu^k \in \overline{\mathcal{U}}} E\left\{ \left(\frac{d\ell(D_i; \alpha_0)}{d\theta^k} - \frac{d\ell(D_i; \alpha_0)}{dh}[\mu^k] \right)^2 \right\}$$

$$= \inf_{(\mu_1, \mu_2, \mu_3)^T \in \overline{\mathcal{U}}} E\left\{ \left(\begin{array}{c} \frac{d\ell(D_i; \alpha_0)}{d\theta^k} - \frac{d\ell(D_i; \alpha_0)}{df_1}[\mu_1] \\ - \frac{d\ell(D_i; \alpha_0)}{df_2}[\mu_2] - \frac{d\ell(D_i; \alpha_0)}{df_3}[\mu_3] \end{array} \right)^2 \right\}.$$

This equation also defines $\frac{d\ell(D_i; \alpha_0)}{dh}[\mu^*]$. Then $\mathcal{S}_{\theta_0} \equiv \frac{d\ell(D_i; \alpha_0)}{d\theta^T} - \frac{d\ell(D_i; \alpha_0)}{dh}[\mu^*]$ becomes the semiparametric efficient score for θ_0, and

$$I_* \equiv E\left[\mathcal{S}_{\theta_0}^T \mathcal{S}_{\theta_0}\right] = V_* \tag{27}$$

becomes the semiparametric information bound for θ_0.

Finally, we can show that the sieve MLE $\widehat{\theta}_n$ is asymptotically normally distributed around θ_0 as follows:

Theorem 3 Suppose that Assumptions of Lemma 1, and Assumptions 11–19 hold. Then: $\sqrt{n}(\widehat{\theta}_n - \theta_0) \xrightarrow{d} N(0, V_*^{-1}I_*V_*^{-1})$, with V_* defined in equation (25) and I_* given by equation (27).

C   Estimation, Simulation, and Robustness Checks

In this section, we provide more details on estimation, conduct simulation exercises to confirm our estimation strategy, and do a number of robustness checks with respect to data and specification.

C.1   Estimation Details

As mentioned in Section 4.3, the nonparametric densities in the sieve MLE estimator are approximated by finite dimensional parametric representations, where the dimension depends on the sample size. We find that Hermite orthogonal polynomials work well as basis functions with just a few sieve terms.[23] Given the sample size of our data sets, we conduct simulation studies in the next subsection to choose the smoothing parameters in our sieve MLE estimator. With a sample size similar to the DMSP/OLS sample, our simulation studies show that the estimates are stable with the number of sieve terms used for each density function being around 6. As such we choose 6 for the DMSP/OLS sample. The VIIRS sample has much fewer observations and we reduce the number of sieve terms to 4.

C.2   Simulations

We consider a data generating process similar to equations (1) and (2) with a quadratic nighttime light production function. There are six equal-sized groups of countries based on statistical capacity ($s_i = 1, 2, 3$) and location ($l_i = 1, 2$). Each group's true GDP distribution follows a mixture of two normal distributions. Measurement errors in both GDP per capita and nighttime lights follow normal distributions where the variances $\sigma(s)$ and $\sigma(l)$ differ for different groups. The quadratic function $m(\cdot)$ is assumed to have the same coefficients as point estimates in the DMSP/OLS data. In the simulation, we draw 400 samples with size $n = 4000$. Table 16 shows the parameter details in the simulations.

Table 17 presents the simulation results with different choices of the number of orthogonal Hermite terms. The coefficients of the quadratic production function are accurately estimated around $k = 6$. For this reason, we apply $k = 6$ to DMSP/OLS data and $k = 4$ to VIIRS data since the latter has much less observations.

To give an idea of how well orthogonal Hermite series approximate density functions, Figure 14 shows an example of the approximated density functions of measurement errors in GDP per capita in one of the simulations ($k = 6$). The approximation is broadly in line with the true distributions.

In Section 4.4, we proposed two new measures of real GDP per capita: the optimal linear measure and the semiparametric conditional mean. While the latter makes full use of the information in the conditional distributions, its nonparametric feature

---

[23]Compared to Hermite polynomials, the drawback for Legendre polynomials is that they have bounded support while Fourier series require many more sieve terms to approximate density functions well.

Table 16: Parameterization in Simulations

Group	y^*	$\sigma(s)$	$\sigma(l)$
1	$0.6N(-0.8, 0.6^2) + 0.4N(0.8, 0.7^2)$	0.4	1
2	$0.7N(-1, 0.9^2) + 0.3N(0.7, 0.8^2)$	0.4	0.8
3	$0.4N(-0.1, 0.6^2) + 0.6N(0.2, 0.8^2)$	0.3	1
4	$0.2N(-0.4, 0.7^2) + 0.8N(0.6, 0.7^2)$	0.3	0.8
5	$0.3N(-0.2, 0.8^2) + 0.7N(1, 0.6^2)$	0.1	1
6	$0.5N(-1, 1) + 0.5N(-0, 4, 0.6^2)$	0.1	0.8

Table 17: Simulation Results

$m(y^*) = \theta_0 + \theta_1 y^* + \theta_2 (y^*)^2$			
Parameter	θ_0	θ_1	θ_2
True values	0.398	1.234	-0.244
$k = 4$	0.364	1.343	-0.229
	(0.083)	(0.075)	(0.065)
$k = 5$	0.370	1.334	-0.234
	(0.039)	(0.047)	(0.030)
$k = 6$	0.365	1.328	-0.227
	(0.041)	(0.111)	(0.030)
$k = 8$	0.357	1.311	-0.221
	(0.091)	(0.140)	(0.058)

Standard errors are based on 400 sample bootstraps.

nonetheless makes it less robust because it requires a large sample size to perform well. In the sparse area of the empirical distribution of $(y_{i,t}, z_{i,t}, s_{i,t}, l_i)$, the semiparametric conditional mean can be volatile, while the optimal linear measure remains robust. In the area where the density $f(y_{i,t}, z_{i,t}, s_{i,t}, l_i)$ takes a relatively larger value, the conditional mean is actually stable and also close to the optimal linear measure.

Graph (a) of Figure 15 contrasts the difference between the semiparametric conditional mean and the optimal linear measure $(E[y_{i,t}^*|y_{i,t}, z_{i,t}, s_{i,t}, l_i] - \hat{y}*)$ against the empirical kernel density estimates of $f(y, z, s, l)$ in the simulated data. Notice that the the difference between the semiparametric conditional mean and the optimal linear measure decreases as the empirical density increases. Meanwhile, we actually observe the true value $y_{i,t}^*$ in the simulation. Graph (b) and (c) show scatter plots of the opti-

Figure 14: Example of Density Function Approximation

(a) Low Capacity   (b) High Capacity   (c) High Income
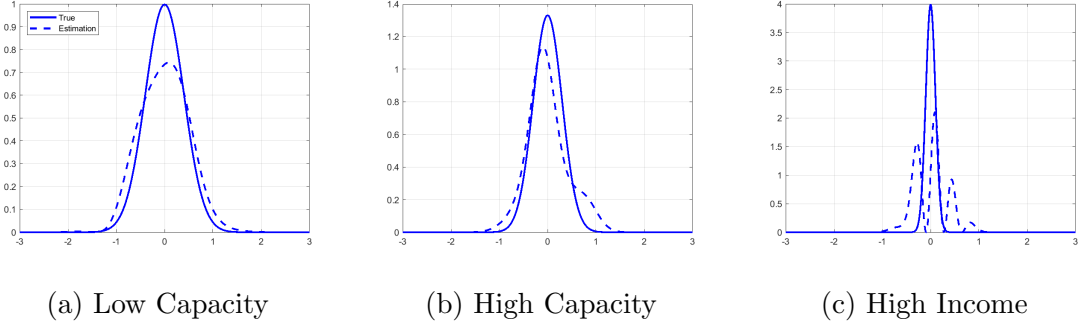
mal linear measure and the semiparametric conditional mean against the true values, respectively. Our new measures perform very well in terms of predicting the true value $y_{i,t}^*$. The mean squared error for the optimal linear measure is slightly smaller but very close to that of the semiparametric conditional mean in the simulation.

For these reasons, we make the optimal linear measure our choice of the new measure for the true GDP.

C.3   Alternative Specifications

We consider a number of alternative specifications of the model.

First, we consider cases where the nighttime lights production function $m(\cdot)$ could be linear or cubic. As suggested by Table 6, the quadratic term is statistically significantly different from zero. However, if we impose that the production function is linear, the estimation results in high income countries having the highest measurement errors. Figure 16 shows that under the linear specification, deviations from the nighttime lights production function are wrongly attributed to measurement errors in official GDP. While the linear specification is mis-specified, the cubic term is not significantly different from zero and it results in unstable performance of the model.

Second, we consider more parametric specification of the error terms in equations (1) and (2). In particular, we assume $\epsilon_{i,t}^y(s_i) = \sigma(s)\epsilon_{i,t}^y$ and $\epsilon_{i,t}^z(l_i) = \sigma(l)\epsilon_{i,t}^z$. In other words, the distribution of measurement errors is the same up to a change of variance for all three groups of countries with different statistical capacity, and similarly for measurement errors in nighttime lights. This specification has the advantage of having less parameters to estimate. Using the same number of sieve terms $k = 6$ for the error terms as in our baseline specification (1) and (2), we obtain similar results, as shown in Figure 17 and Table 18. However, we find this specification to be less robust to the choice of the number of sieve terms despite its parsimonious specification. Thus we choose the distribution of measurement errors to be different for countries with different statistical capacity and geographical location groups.

Third, we consider a full parametric specification where the nighttime lights production function is quadratic and the true GDP per capita as well as all measurement errors are normally distributed. Despite being computationally lightweight, the full parametric specification is not very robust to outliers. Using the full sample
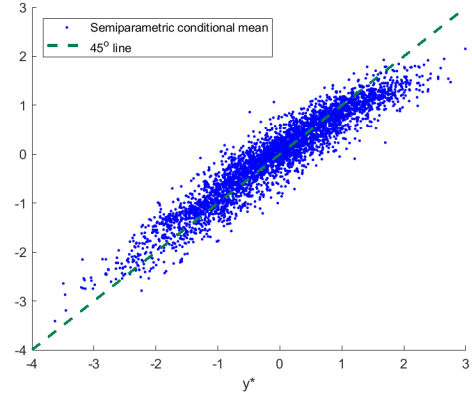
Figure 15: Semiparametric Conditional Mean and Optimal Linear Measure
Performance in Simulations
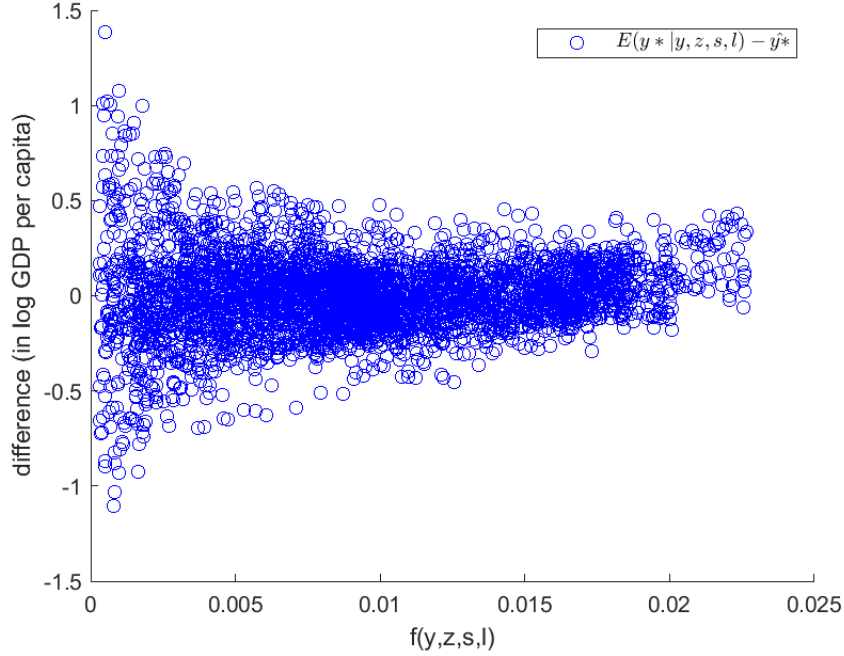
(a) Difference between New Measures
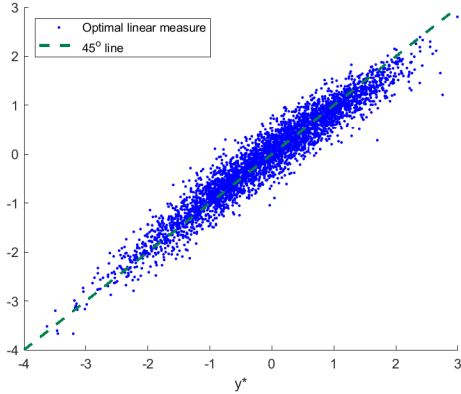
(b) Optimal Linear Measure
vs. True Values

(c) Semiparametric Conditional Mean
vs. True Values

DMSP/OLS sample, we obtain the counterintuitive and incorrect results that high income countries have the highest measurement error, as shown in Table 19. However, if we remove autonomous territories such as Hong Kong and Macau and city states such as Singapore, where nighttime lights per capita was unusually low as a result of high population density, we obtain the more intuitive results that the variance of measurement errors is much smaller for high income countries. In light of this sensitivity, we prefer the semiparametric specification.

Table 18: Estimated Light Production Function (DMSP/OLS)
with Parsimonious Error Structure

$$m(y^*) = \theta_0 + \theta_1 y^* + \theta_2 (y^*)^2$$

Parameter	θ_0	θ_1	θ_2
Point Estimate	0.326	1.261	-0.212
Standard Error	(0.160)	(0.090)	(0.032)

Parameters are estimated using demeaned data. Standard errors are based on 400 sample bootstraps.

Table 19: Full Parametric Specification (DMSP/OLS)

$$m(y^*) = \theta_0 + \theta_1 y^* + \theta_2 (y^*)^2$$

Parameter	θ_0	θ_1	θ_2	σ_1^y (low capacity)	σ_2^y (high capacity)	σ_3^y (high income)
				All Data		
Point Estimate	0.336	1.352	-0.256	0.458	0.474	0.791
Standard Error	(0.047)	(0.034)	(0.041)	(0.025)	(0.020)	(0.056)
				Excluding Hong Kong SAR, Macau SAR, and Singapore		
Point Estimate	0.316	1.354	-0.268	0.458	0.471	0.050
Standard Error	(0.012)	(0.015)	(0.008)	(0.019)	(0.015)	(0.006)

Parameters are estimated using demeaned data. Standard errors are based on 400 sample bootstraps.
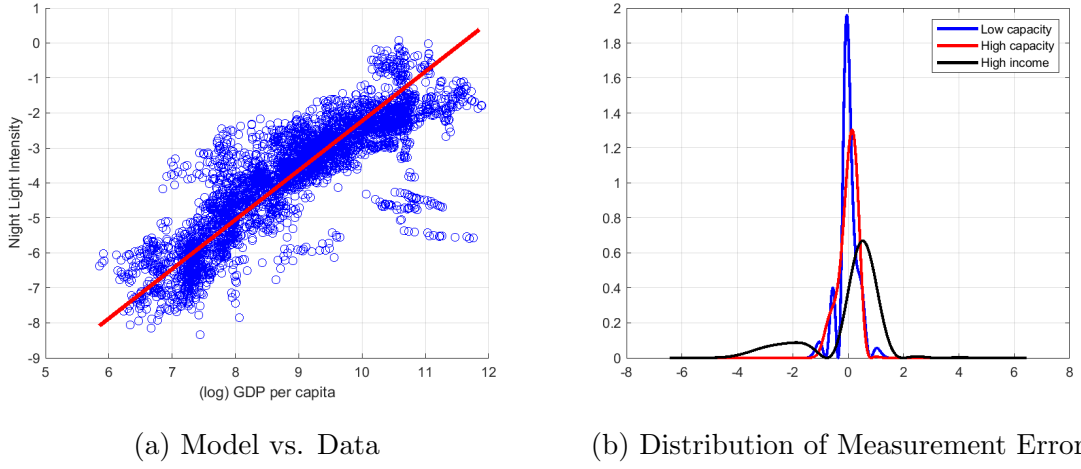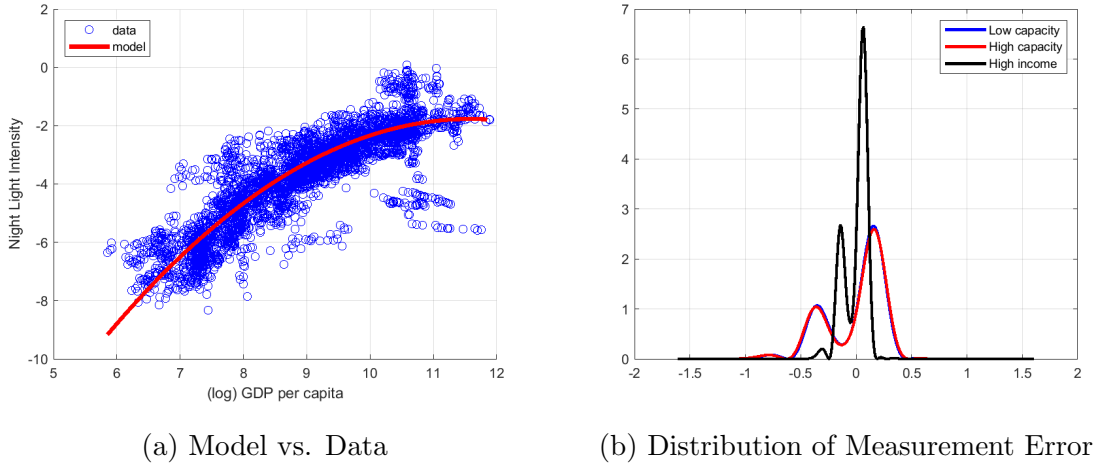
Figure 16: Linear Specification

(a) Model vs. Data

(b) Distribution of Measurement Error

Figure 17: Quadratic Specification with More Parsimonious Error Structure

(a) Model vs. Data

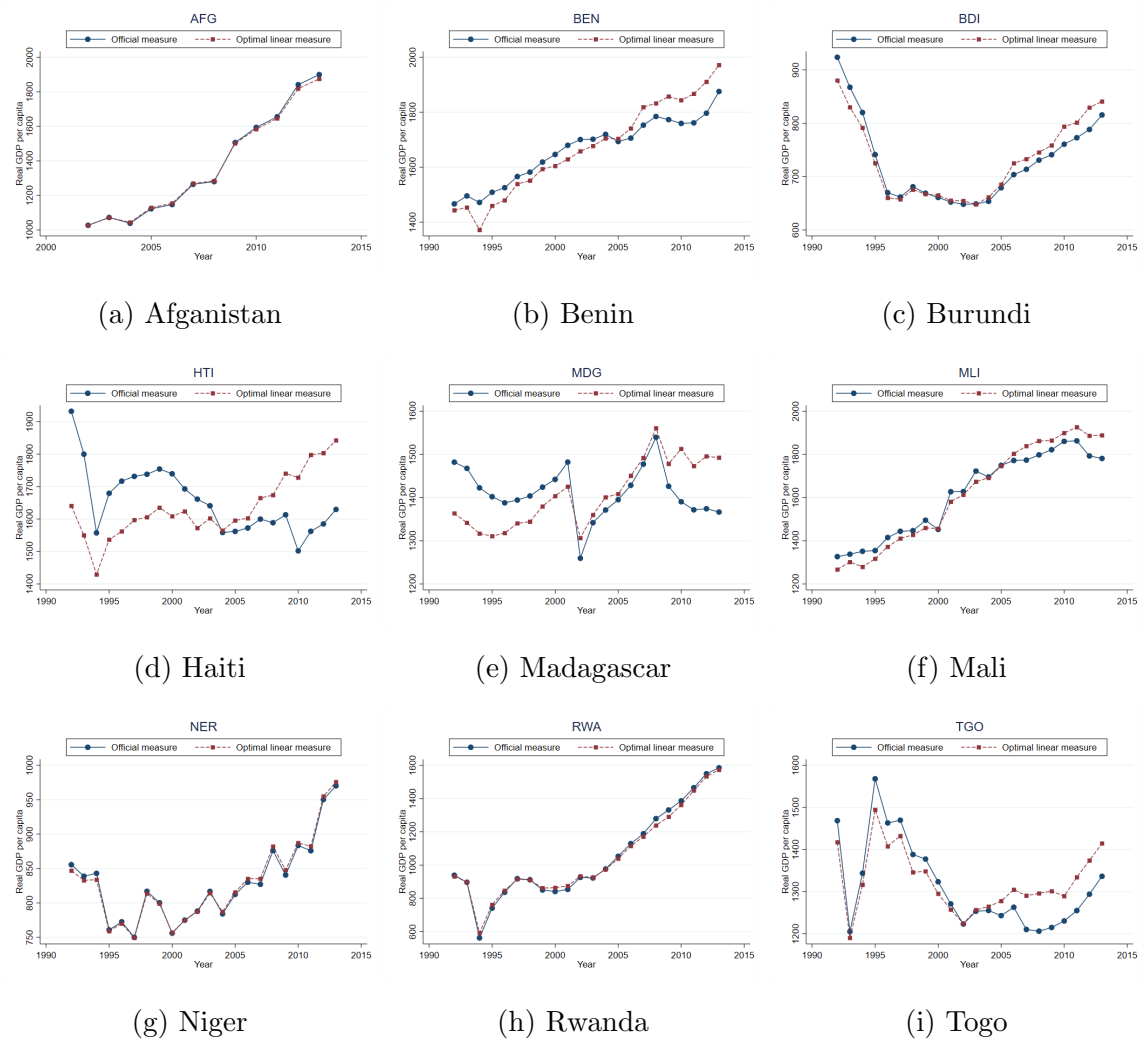(b) Distribution of Measurement Error

Finally, we consider combining the DMSP/OLS and VIIRS datasets by assuming that the measurement errors in official real GDP per capita follow the same distribution in the two datasets. We find that the estimated production functions are similar to our baseline results and there is little change in our new measures of real GDP per capita.

C.4 Optimal Linear Measure for More Countries

Given the high uncertainty about official data in low income countries, we present more results comparing the optimal linear measure of real GDP per capita with official data for a number of low income countries in Figure 18.

Note that the optimal linear measure being close to official data for some low income countries does not necessarily mean the official data are accurate. More often than not, it means nighttime lights for those countries do not contain much information

Figure 18: New Measures for Low Income Countries

(a) Afganistan   (b) Benin   (c) Burundi

(d) Haiti   (e) Madagascar   (f) Mali

(g) Niger   (h) Rwanda   (i) Togo

either as a result of lack of electricity. As such the optimal linear measure puts low weight on nighttime light-predicted GDP. Nevertheless, these estimates show that our proposed optimal linear measure performs very reliably across countries.

C.5 Semiparametric Conditional Mean for Robustness Check

In Section 4.4, we discussed the use of the semiparametric conditional mean as another new measure of real GDP per capita. Despite its clear advantage of making full use of the information in the conditional distributions, its nonparametric feature makes it less robust without a large sample size.

Figure 19 plots the difference between the semiparametric conditional mean and the optimal linear measure $(E[y_{i,t}^*|y_{i,t}, z_{i,t}, s_{i,t}, l_i] - \hat{y}*)$ against the empirical kernel density estimates of $f(y, z, s, l)$ in DMSP/OLS data. Consistent with the simulation results in Appendix C.2, as the empirical density increases, the difference between the semiparametric conditional mean and the optimal linear measure decreases. Note

that the difference is almost zero for high income countries because their measurement errors that are identifiable by our method are very small.

Figure 19: Semiparametric Conditional Mean and Optimal Linear Measure
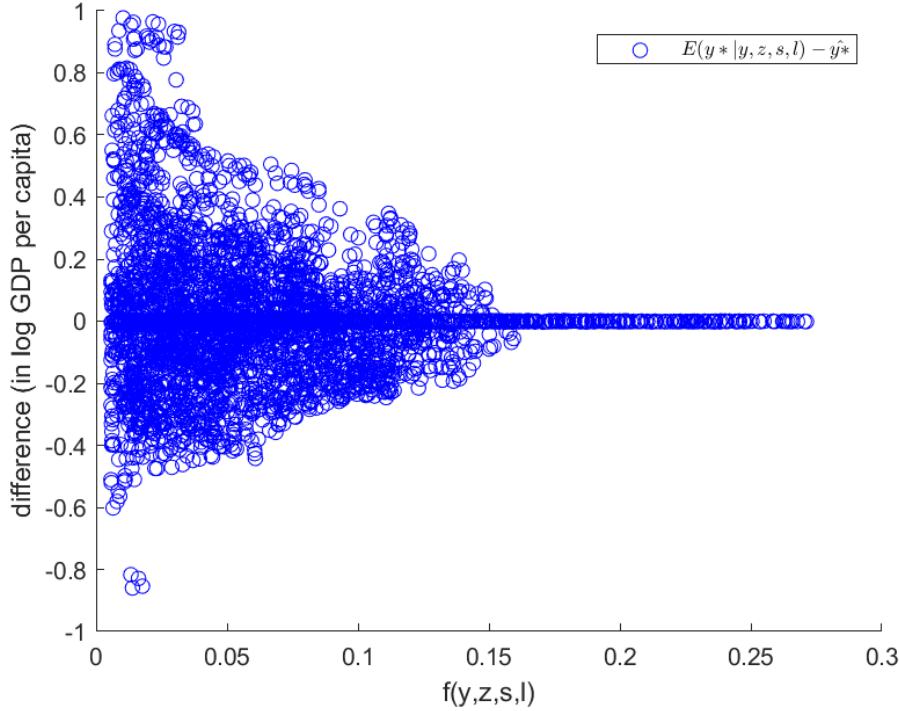
D   More Descriptive Details on Data

D.1   Nighttime Lights vs. Real GDP per capita

Figure 20 presents where countries are located on nighttime lights and real GDP per capita graph. We choose selectively a few countries that together span the real GDP per capita spectrum.

D.2   Statistical Capacity and Latitude

We use the World Bank's Statistical Capacity Indicator[24] for developing countries as our variable s for statistical capacity. The Statistical Capacity Indicator is a composite score assessing the capacity of a country's statistical system, including the following areas: methodology; data sources; and periodicity and timeliness. The scores are based on 25 criteria in these areas and the overall Statistical Capacity score is then being calculated as simple average of all three area scores on a scale of 0-100.

Because the indicator starts in 2004 and the change over time for each country is small, we use the average score during our sample periods for each country. Since

---

[24]http://datatopics.worldbank.org/statisticalcapacity/

Figure 20: Nighttime Lights vs. Real GDP per capita (1992-2013)
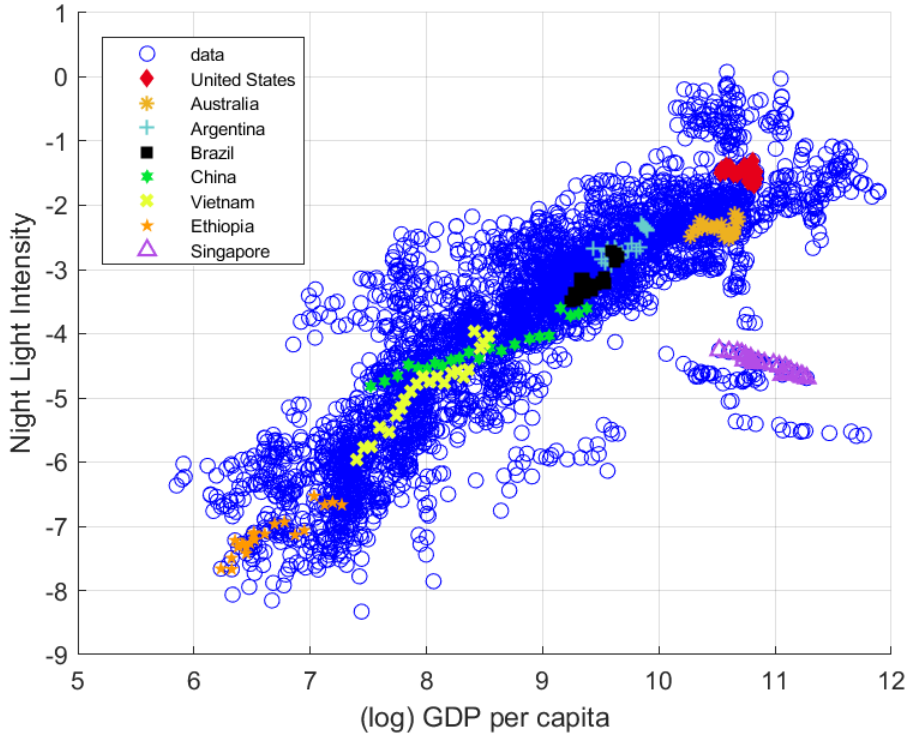
high income countries don't have scores, we assign them the highest score and treat them as a separate group. Figure 21 shows that there is a clear positive relationship between real GDP per capita and statistical capacity. Note that high income countries are located on the top right corner where statistical capacity is 100 by construction.

A country's latitude is calculated as the centroid of its largest contiguous block. We focus on contiguity because oversea territories or separate land blocks would complicate the definition of the geographic center of a country. As an example, Figure 22 illustrates the centroids that we use for a few European countries. Figure 23 shows that real GDP per capita varies with latitude. Countries at high latitude in both the Northern and the Southern Hemispheres tend to be rich whereas countries at low latitude tend to be poor. This is the well-known North-South Divide.

Collectively, Figure 21 and 23 indicate that Assumption 5 is fairly reasonable, i.e., the distribution of real GDP varies with countries' statistical capacity and geographic location.

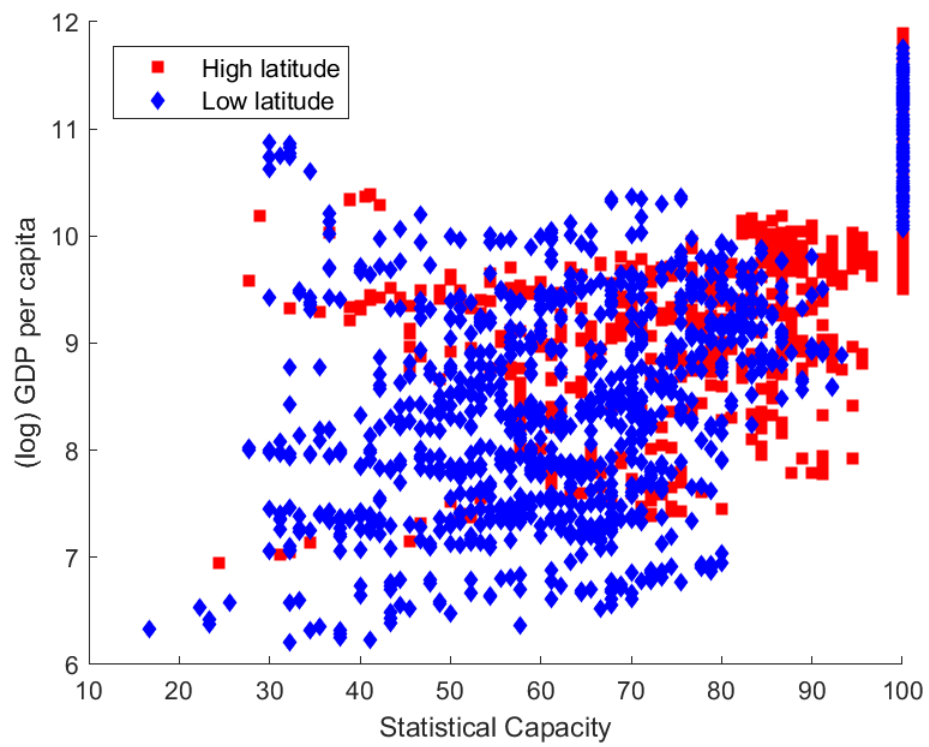Figure 21: Real GDP per capita vs. Statistical Capacity by Location (1992-2013)

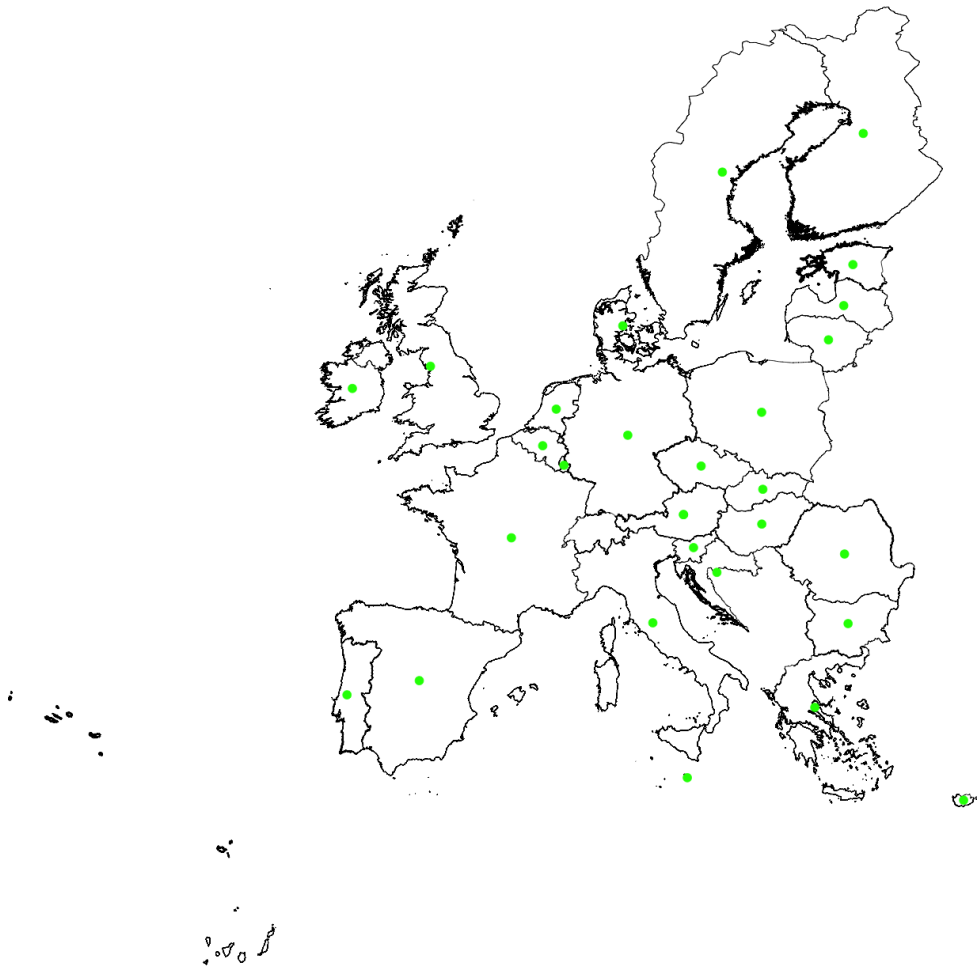Figure 22: Centroids of Selected European Countries

Figure 23: Real GDP per capita vs. Latitude by Statistical Capacity
(1992-2013)